2017

Study of Stability and Thermal Conductivity of Nanoparticles in Propylene Glycol

Sumit Mahajan
Minnesota State University, Mankato

Recommended Citation

Mahajan, S. (2017). Study of Stability and Thermal Conductivity of Nanoparticles in Propylene Glycol [Master's thesis, Minnesota State University, Mankato]. Cornerstone: A Collection of Scholarly and Creative Works for Minnesota State University, Mankato. https://cornerstone.lib.mnsu.edu/etds/676/

Study of Stability and Thermal Conductivity of Nanoparticles in Propylene Glycol

A Thesis Submitted in Partial Fulfillment of the

Requirements for the Degree of

Master of Science in Mechanical Engineering

Minnesota State University, Mankato

By

Sumit Mahajan

June 2016

03/22/2017

Study of Stability and Thermal Conductivity of Nanoparticles in Propylene Glycol

Sumit Mahajan

This thesis has been examined and approved by the following members of the student's committee.

Advisor (Dr. Patrick Tebbe)

Committee Member (Dr. Sungwon S. Kim)

Committee Member (Dr. Namyong Lee)

Acknowledgement

It is with immense gratitude that I acknowledge the support and help of my advisor, Dr. Patrick Tebbe in completing my thesis. He has motivated and inspired me to work on this project. It wouldn’t be possible to finish this project without his guidance, expertise and all the resources which I have loaned from him. I also want to thank Dr. Sungwon S. Kim and Dr. Namyong Lee for being part of my committee and giving valuable inputs on my thesis. I would also like to thank Mr. Kevin Schull for helping me with the lab equipment and setting up my lab experiments. I also want to thank my friends Divi, Raka Paul and Jaysimhna for help me with the mathematic part of my research. Lastly, I would like to thank my family, they are the reason that I have made it this far academically and in life as well.

Table of Contents

List of Figures

Nomenclature

σ– yield stress

H- hardness

d- nanoparticles diameter

k_h- slope

ε– strain rate

D- diffusion coefficient

G- shear modules

b- burger’s vector

F_D- drag force

J- flux of particles

Cc- Cunningham correction factor

Kb- Boltzmann’s constant

T- temperature

Kth- thermophoretic diffusion coefficient

η– viscosity

β – proportionality factor

τ– shear factor

ϕ– volumetric concentration

F- force

A- area

p- nanoparticles subscript

b- base fluid subscript

Ψ– shape factor

List of Tables

Abstract

Title of Thesis: Study of Stability and Thermal Conductivity of Nanoparticles in Propylene Glycol

Degree Candidate: Sumit Mahajan

Degree: Master of Science in Mechanical Engineering 2016

Minnesota State University, Mankato, MN

This thesis studied the effects of gravity induced settling, thermophoresis and Brownian motion on the thermal conductivity of the Aluminum Oxide (Al_2O_3) nanofluids. The base fluid was propylene glycol. The effects were studied by making three samples with volumetric percentages of 0.2 %, 2% and 3% Al_2O_3 in propylene glycol. Sets of 22 experiments were conducted over time to understand the behavior of settling. All samples were manually mixed each time the experiment was conducted. A Thermtest Transient Plane Source TPS 500S was used to measure the thermal conductivity. Volumetric percentages and diameters of nanoparticle were chosen so that the effect of coagulation was minimized. The diameter of nanoparticle chosen was 15nm. The maximum thermal conductivity enhancement happened when the volumetric percentage of 3% Al_2O_3 was added in propylene glycol. It was also concluded in our experimental setup, that gravity significantly affected the settling of nanoparticles.

Chapter 1

Introduction

A nanofluid is a suspension of nanometer- size particles in a fluid. With the addition of nanoparticles to the base fluid, changes in properties of the new fluid occurs. The properties that change are viscosity, density, and thermal conductivity. Thermal conductivity is the most important of the properties to study. Many researchers have shown that thermal conductivity increases when nanoparticles are added in the right proportion to the base fluid. These results are not repeatable over time since nanoparticles settle due to gravity. Efforts have been made to make stable nanofluids in which particles are well dispersed. Some of the efforts made to ensure stable well dispersed mixture were the use of surfactants, smaller diameter nanoparticles, and vibration.

The aim of this research was to study the stability of the nanoparticles in the fluid. A stable nanoparticle mixture is one in which the nanoparticles are well dispersed, even with the passage of time. Nanoparticle chosen for study was aluminum oxide (Al_2O_3) and diameter was 15 nm. The study of gravity, Brownian motion, and thermophoresis in the nanofluid help in understanding the stability of nanofluids. The aim of the experiments was to study the effects of gravity, Brownian motion, ` and thermophoresis on the settling of nanoparticles. Volumetric concentrations were kept below 3% to make sure the coagulation effect was minimized.

Chapter 2

Background and Literature Review:

2.1 Background:

Extensive research on the use of nanoparticles is being done across the world to study the enhancement in the thermal properties of base fluids. A new class of fluid is engineered by suspending nanoparticles in the conventional heat transfer fluids; these fluids are called nanofluids. Nanofluids have a wide range of applications, some of their applications include being used in an automobile transmission, drilling fluids, HVAC, coolant oils etc. Several studies have been done on nanofluids, which indicates that nanoparticles help in improving the thermal properties of the fluids. Studies have shown that thermal conductivity and density help in improving the heat transfer coefficient of the fluid.

Liquid cooling is an effective way of removing a high heat load from components. Liquid cooling is used when air cooling is no longer providing enough heat removal [1], [2]. There are two types of liquid cooling: contact cooling and cabinet cooling. A liquid cooling loop usually consists of a cold plate, pump, heat exchanger, and pipes. Liquid flows through the loop, extracting heat from the hot source and dissipating heat out in ambiance resulting in maintaining the parts at the desired temperature. Liquid cooling is used to cool high power devices within many industries such as medical and defense, laser, data centers, semiconductor, transportation, printing and more.

Researchers are working on improving the efficiency of the cooling liquid-coolants. The most commonly used coolants for liquid cooling applications today are water, deionized water, glycol and water solutions and Dielectric Fluids [2]. Water is a good choice to be used as coolant due to its high specific heat and high thermal conductivity, but, one disadvantage is that it corrodes the metal. Two kinds of glycols commonly used for liquid cooling applications are ethylene glycol and water (EGW) and propylene glycol and water (PGW) solutions. Ethylene glycol has desired thermal properties which include a high boiling point, a low freezing point, and stability over a large range of temperatures, high specific heat, and thermal conductivity. But, ethylene glycol is toxic in nature. Propylene glycol is considered safe for use in food or food processing applications and can be used in enclosed spaces [2]. In engine coolants, propylene glycol is used to reduce the freezing point of the liquid, thus, preventing the engine from corrosion, overheating and freezing. Another property of propylene glycol is that it retains its flowability and does not create added pressure in pipes or vessels. It makes propylene glycol the ideal solution for burst protection in pipe and containment systems [3]. Its applications are in pipes and tubes, solar panel systems, temperature sensitive use with engines, or under extreme conditions and marine transportation. Another specific property of propylene glycol is that it can reduce the freezing point of water to -60^{o}C, depending on dilution. Also, it is non- toxic, easily biodegradable, non- corrosive to metals, non- flammable, and easy to handle.

To increase the efficiency of cooling liquid, heat transfer rate need to be enhanced. Various studies have shown that addition of nanoparticles has enhanced the heat transfer rate of the fluids. K. S. Suganthi et al. [4] had conducted an experiment with propylene glycol/ ZnO nanofluids. The result was the enhancement of thermal conductivity by 26%. Although researchers have found improvement in thermal conductivity of nanofluids, these results are not repeatable over time [5], [6], [7]. The reason for this behavior is the set [8]tling and clustering of the nanoparticles in the fluids. Gravitation, Brownian motion and thermophoresis has effects on the settling of the nanoparticles in nanofluids. My aim is to study the behavior of gravity induced settling, Brownian motion and thermophoresis on thermal conductivity and the stability of the nanofluids.

2.2 Propylene Glycol:

Propylene glycols play a significant role in the industry due to its wide range of practical application. The versatile performance of propylene glycol is antifreeze/ coolant formulations, heat transfer fluids, solvents, food, flavors and fragrances, cosmetics and personal care products, pharmaceuticals, chemical intermediates, hydraulic fluids, plasticizers, resin formulations, gas dehydration operations and much more. The structural formula of propylene glycol is:

$$CH_3\overset{\overset{OH}{|}}{C}H-\overset{\overset{OH}{|}}{C}H_2$$

Figure 1 Formula of Propylene Glycol [3]

Glycol is an aliphatic organic compound having two hydroxyl groups per molecule. Glycols resemble water; they are clear, colorless liquids with practically no odor. Glycols are excellent solvents for many organic compounds and are completely water soluble. The properties of propylene glycol are given in table 1 [8]:

Table 1: Physical properties of propylene glycol *[8]*

Physical	Units	
Chemical Name		1,2-propanediol
Formula		$C_3H_8O_2$
Molecular Weight	grams	76.1
Boiling point	760 mm Hg, ^oF	369.3
	760 mm Hg, ^oC	187.4
Vapor Pressure	Mm Hg, 77^oF (25^oC)	0.13
Evaporation Rate	(n- Butyl Acetate =1)	1.57E-02
Density	g/cm^3, 77^oF (25^oC)	1.032
	g/cm^3, 140 ^oF (60 ^oC)	1.006
	Lb/gal, 77^oF (25^oC)	8.62
Freezing Point	^oF (^oC)	Supercool
Pour Point	^oF	<-71
	^oC	<-57
Viscosity	Centipoise (mPas),	48.6
	Centipoise (mPas),	8.42
Surface Tension	Dynes/cm (mN/m),	36
Refractive Index at 77		1.431
Specific Heat	Btu hr-1 ft-1, 77 ^oF	0.60
	J/g/K, 25^oC	2.51
Flash Point	^oF (^oC)	220.2 (104)
Dipole Moment	Debyes	3.60
Coefficient of		7.3×10^{-4}
Thermal Conductivity	Btu hr-1 ft-1 ^oF-1,	0.1191
	W/m*K, 25^oC	0.206
Heat of Formation	Kcal/g-mol	-101
	KJ/mol, 25^oC	-422
Heat of Vaporization	Btu/lb, 77 ^oF	379
	KJ/mol, 25^oC	67
Electrical	Mhos/cm (S/cm),	0.1×10^{-6}

2.3 Nanoparticles:

Nanoparticles are particles with a diameter of 1 to 100 nanometers. Nanoparticles can be metals, alloys, semiconductors, ceramics, glasses, polymers, and inorganic carbon-based materials. Nanoparticles can be oxides, carbides, nitrides or borides. Some examples of oxide nanoparticles are Aluminum Oxide (Al_2O_3), Magnesium Oxide (MgO), Cerium Oxide (CeO_2), Ferrous Oxide (Fe_2O_3), Copper Oxide (CuO) etc. Oxide nanoparticles exhibit unique physical and chemical properties due to their limited size and a high density of corner or edge surface sites [9].

2.4 Motion in Nanofluids:

Nanoparticles in nanofluids develop motion with respect to the base fluid. Various phenomenon and external forces are the reason for the development of the motion of nanoparticles. Some of the effects are gravity, Brownian motion, thermophoresis, convection, magnetic flux, electric flux etc. From the previous studies: gravity induced settling, Brownian motion, and thermophoresis played an important role in the motion in nanofluids.

2.4.1 Gravity:

To get familiarized with the effect of gravity, it is important to understand steady – straight line motion [10]. The uniform motion is the result of the action of two forces, first is a constant external force which can be either gravitational force or some electrical force and the resistance offered by the fluid to the particles [11]. Aerosol particles come to a constant velocity almost instantly. Hence, it is important to study uniform particle motion.

The resisting force of the gas depends on the relative velocity between the particle and the gas and is the same whether the particle moves through the gas or the gas flows past the particle [12], [13].

Newton had derived the force resisting the motion of a sphere passing through a gas. Newton's resistance law is valid for Reynolds number greater than 1000. Newton reasoned that the resistance experienced by the sphere traveling in the gas is the result of the acceleration of the gas that must be pushed aside to allow the sphere to pass through [14]. The mass of the air pushed by the sphere can be given by the equation:

$$\dot{\mathrm{m}} = \rho_g \frac{\pi}{4} d^2 V \tag{1}$$

The change in momentum per unit time is given by:

$$\frac{change\ of\ momentum}{unit\ time} = \rho_g \frac{\pi}{4} d^2 V^2 \tag{2}$$

The change in momentum is equal to the force required to move the sphere through the gas. It is called a drag force and is given by:

$$F_D = C_D \frac{\pi}{8} \rho_g d^2 V^2 \tag{3}$$

2.4.2 Stokes law:

Aerosols have low velocities and small particle sizes. Hence, aerosols have low Reynolds numbers. Newton’s resistance law is applied to the situations where Reynolds number is more than 1000. Aerosols have low Reynolds numbers, which means viscous forces are more predominant in an aerosol. In 1851, Strokes derived the expression for drag at the other extreme, when inertial forces are negligible compared to viscous forces [12]. Stroke law is a solution to the generally unsolvable Navier- Stokes equations. [15] These equations are the general differential equations describing fluid motion [12], [16], [17].

Stokes gave the total resisting force acting on a spherical particle moving with a velocity V through a fluid [12]:

$$F_D = 3\pi \eta \mathrm{Vd} \tag{4}$$

Stokes law includes viscosity, but not factors associated with inertia, such as the density of gas; Newton’s law contains density, but not viscosity.

2.4.3 Settling Velocity and Mechanical Mobility:

Settling velocity can be derived by Stokes law. When particles are released, they reach their terminal velocity, a condition in which drag force on the particle is equal and opposite to the force of gravity.

It is given by equation [12]:

$$F_D = F_G = mg \tag{5}$$

$$3\pi\eta V d = \frac{(\rho_p - \rho_g)\pi d^3 g}{6} \tag{6}$$

Solving the above equation for the terminal settling velocity V_{TS} gives:

$$V_{TS} = \frac{\rho_p d^2 g}{18\eta} \tag{7}$$

But the above equation is valid for the diameter of the particles above 1 µm and Re less than 1.0 [12].

An important assumption of Strokes law is that the relative velocity of the gas right at the surface of the sphere is zero. This is not true when the particles are nanoparticles and size approaches the mean free path of the gas. These particles settle much faster than expected because there is “slip” at the surface of the particle. Cunningham derived a correction factor for Strokes’ law. The factor, called the Cunningham correction factor C_c, is always greater than one and reduces the Strokes drag force by [12]:

$$F_D = \frac{3\pi\eta V d}{C_c} \tag{8}$$

$$C_c = 1 + \frac{\lambda}{d}\left(2.34 + 1.05\exp(-0.39\frac{d}{\lambda}\right) \tag{9}$$

The slip- corrected form of the terminal settling velocity is given by:

$$V_{TS} = \frac{\rho_p d^2 g C_c}{18\eta} \tag{10}$$

This equation is valid for all particle sized when Re<1.0.

2.4.4 Brownian Motion:

Brownian motion is the phenomenon which was first observed by botanist Robert Brown in 1827. He observed the continuous wiggling motion of pollen grains in water that we call Brownian motion now [12]. In the 1900s, Einstein derived the relationships characterizing Brownian motion. Brownian motion is the irregular wiggling motion of an aerosol particle in the still air caused by random variations in the relentless bombardment of gas molecules against the particle. Diffusion of aerosol particles is defined as the net transport of these particles in a concentration gradient. The transportation is from higher concentration to lower concentration. The process is characterized by the particle diffusion coefficient D. The larger the value of D, the more vigorous the Brownian motion and the more rapid the mass transfer in the concentration gradient [12]. The diffusion coefficient relates the flux J of aerosol particles and the concentration gradient dn/dx. The relationship is known as Fick's law and is given by:

$$J = -D\frac{dn}{dx} \tag{11}$$

According to Stokes- Einstein derivation, the diffusion force on the particles, which causes their net motion down the concentration gradient is equal to the force exerted by the gas resisting the particles' motion. Hence, diffusion force can be given by:

$$\mathrm{diffusion\ force} = \mathrm{F_{diff}} = \frac{3\pi\eta \mathrm{Vd}}{\mathrm{C_c}} \qquad (12)$$

Einstein observed that the diffusion force on a particle is the net osmotic pressure force on the particle [12]. The osmotic pressure P_o is given by Van't Hoff's law for n suspended particles per unit volume,

$$P_o = kTn \qquad (13)$$

The diffusion coefficient after comparing Stokes- Einstein derivation and Van's Hoff's law is given by equation:

$$D = \frac{kTC_c}{3\pi\eta d} \qquad (14)$$

Diffusion coefficient had units of m^2/s. It increases with temperature. Not only does the diffusion coefficient of a particle characterize the intensity of its Brownian motion, but it is also equal to the rate of particle transport in a unit concentration gradient [12]. Thus, a 0.01 µm particle will be transported by diffusion 20,000 times faster than a 10 µm particle [12].

2.4.5 Thermophoresis:

Thermophoretic force is the force that results because of the temperature gradient in the fluid. Nanoparticles in the fluid experience this force in the direction of the decreasing temperature [18]. The magnitude of the force depends on fluid, particle properties, and temperature gradient [19], [20].

The thermophoresis force on a particle is given by:

$$F_{th} = \frac{-p\lambda d^2 \nabla T}{T} \tag{15}$$

The thermophoresis velocity is given by:

$$V_{th} = \frac{-0.55\eta \nabla T}{\rho_g T} \tag{16}$$

V_{th} is independent of particle size and is directly proportional to the temperature gradient [12], [21] .

For the thermophoretic velocity of nanofluids, McNab and Meisen [22] introduced a similar equation where the thermophoretic coefficient is replaced by a proportionality factor β [23], [24], [25].

$$V_t = -\beta \frac{\mu_f}{\rho_g} \frac{\nabla T}{T_g} \tag{17}$$

$$\beta = \frac{k}{2k + k_p} \tag{18}$$

It is very difficult to accurately measure the effects of thermophoresis. To get reliable results it is important to eliminate the effects of gravity, Brownian motion, and natural convection [26]. Gravity's effects can't be eliminated. The gravitational effect changes with the diameter and/or density of the particle [26]. To get an accurate measurement of thermophoretic effects, the diameter of particles must be small and only one fluid should be used so that gravitational effect is eliminated. Cai at el[26] found out that particle velocity becomes larger as particle diameter becomes smaller [27], [28], [29].

Chapter 3: Theory

3.1 Thermal Conductivity and Nanoparticles:

The primary limitation in the development of energy efficient heat transfer fluids is low thermal conductivity of the fluids. A new class of fluids can be engineered by suspending metallic nanoparticles in the conventional heat transfer fluids [30], [31], [32]. These fluids are known as Nanofluids. Nanofluids are expected to exhibit higher thermal transportation properties than the basic conventional heat transfer fluids. They represent the best hope for enhancement of heat transfer [33].

Table 2: Thermal conductivity of different materials

Material	**Thermal Conductivity (W/m.K)**
Metallic Solids	
Silver	429
Copper	401
Aluminum	237
Nonmetallic Solids	
Silicon	148
Metallic Liquids	
Sodium @ 644 K	72.3
Nonmetallic Liquids	
Water	0.613
Engine oil	0.145

From Table 2, the thermal conductivity of copper at room temperature is nearly 700 times greater than that of water and nearly 3000 times greater than engine oil. Furthermore, since there is such a big difference in the thermal conductivity values, it is expected that the thermal conductivity of fluids containing suspended solid metallic particles is higher when compared with the conventional heat transfer fluids [33]. The research in this field had started by dispersing micrometer- sized particles in the fluids but, the results were not good enough and it also resulted in clogging the flow of passages. Nanoparticles have larger surface area and therefore have a great potential for application in heat transfer. Nanoparticles are small enough that they are expected to behave like molecules of liquid [33].

Several studies have been done with nanofluids and the results have been reported by researchers. Most of the studies are done by using oxide nanoparticles such as Al_2O_3, CuO, ZnO, Fe_3O_4, MgO and TiO_2 in base fluid [34]. Das et al. [35] measured the thermal conductivity of Al_2O_3 and CuO with base fluid as water at different temperatures and concentrations. The conclusion of the study was that, with increasing temperature and concentration thermal conductivity can be enhanced by 24.3% to the base fluid. Chon et al. [36] investigated the thermal conductivity of Al_2O_3 nanofluid by using transient hot wire method. The temperature range in the study was between 21^oC and 71^oC and nanoparticles diameter is from 11 nm to 150 nm. The result was that with the increase in the particle size thermal conductivity decreases. Murshed et al. [37] determined the thermal conductivity of TiO_2/ water nanofluid by using spherical rod-shaped nanoparticles. The enhancement in thermal conductivity was 30% for spherical particles and 33% for the rod-shaped nanoparticles.

Li and Peterson [38] studied the effect of nanoparticle diameter on the thermal conductivity. They concluded that by keeping the volume fraction constant at 6% and increasing the diameter of nanoparticle from 36 nm to 47 nm thermal conductivity reduces from 28% to 26%. Zhang et al. [39] did an experiment to find thermal conductivity of various nanofluids. He compared the values with the results found by mathematical calculations. The conclusion was that the values obtained by both the procedure were nearly same. Sundar et al. [40] reported the thermal conductivity of Fe_3O_4/ water in the temperature range of 20^{o}C to 60^{o}C. The maximum enhancement in thermal conductivity was 48% at 60^{o}C. Lee et. Al. [41] obtained enhancement of 1.44% in the thermal conductivity of Al_2O_3/water when volume concentration was increased from 0.1% to 0.3%. Jahanshahi et al. [42] measured the thermal conductivity of SiO2/water nanofluids with volume concentration from 1% to 4% and particle size of 12 nm. The result was that the thermal conductivity increases with the increase in the volume concentration. Thermal conductivity at 1% and 4% volume concentration was enhanced by 3.23% and 23% respectively. K. S. Suganthi et al. [4] conducted the experiments to find the thermal conductivity improvement in ZnO- propylene glycol nanofluids. Their conclusion was that at a 2 vol. % of ZnO in propylene glycol the improvement in thermal conductivity was 26% compared to base fluid.

From the results of the experiments it is evident that nanoparticles in the right proportion can help in improving the thermal conductivity of the nanoparticles. But, these results are not repeatable over time because of the settling and clustering of the nanoparticles. Efforts have made to form stable nanofluids. One of these efforts is the introduction of surfactants [43], [44]. Guodong Xia et al. [43] worked on the effect of surfactant on the stability and thermal conductivity of Al2O3/ de- ionized water nanofluids. The effect of two kinds of surfactants- sodium dodecyl sulphate (SDS) and polyvinylpyrrolidone (PVP) were studied. The conclusion made was surfactants improved the stability of the nanofluids but by adding them into the fluid thermal conductivity decrease. A similar study has been done by Lifei Chen and Huaqing Xie [44] by adding a cationic gemini surfactant in carbon nanotube nanofluids. Gemini surfactant used to stabilize water-based carbon nanofluids. Results showed to improve the stability but to improve the thermal conductivity the quantity of the added surfactant should be appropriate.

Another approach used to improve the stability of nanofluids is the use of vibrations to keep the particles well dispersed in the fluid [45], [46], [47].

3.2 Understanding TPS:

TPS 500 S is a Thermal Constants Analyzer which quickly and accurately measures the thermal conductivity, thermal diffusivity and specific heat capacity of an extended range of materials. TPS 500 S measures the thermal properties of solids, pastes, gel, and powders. The method to measure thermal conductivity is based on the use of a transiently heated plane sensor and is referred as the Hot Disk Thermal Constants Analyzer. The Hot Disk sensor consists of an electrically conducting pattern in the shape of a double spiral, which has been etched out of a thin metal (Nickel) foil. This spiral is sandwiched between two thin sheets of an insulating material (Kapton, Mica, etc.).

Figure 2: TPS 500S *[48]*

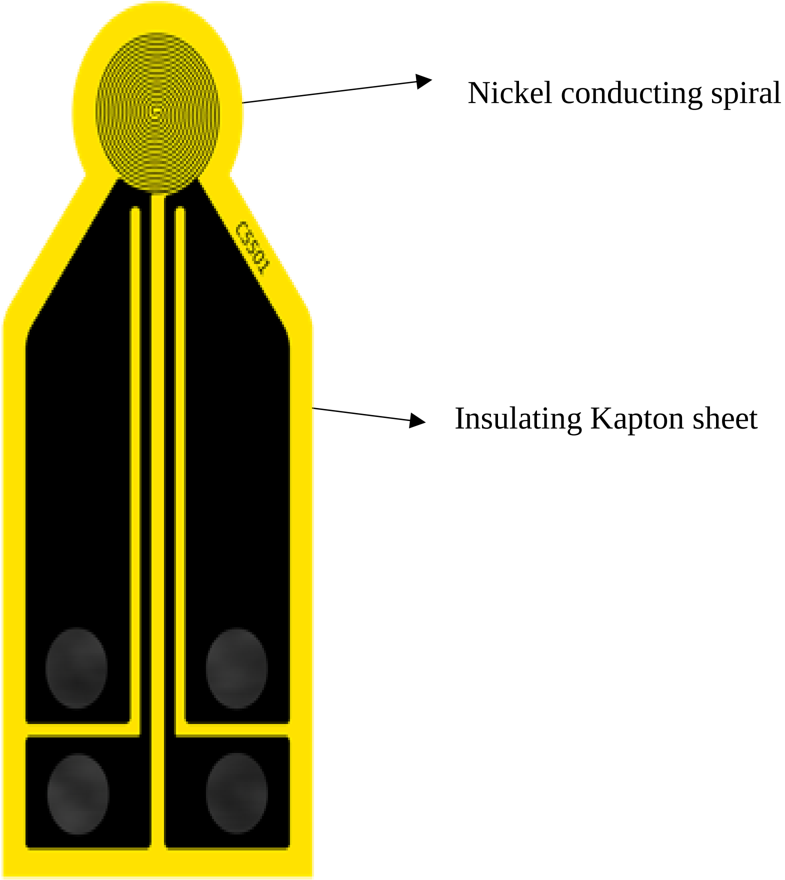

Figure 3 TPS 500 S sensor *[48]*

To perform the thermal transport measurements, the Hot Disk sensor is fitted between two pieces of sample: each one with a plane surface facing the sensor. By passing electrical current high enough to raise the temperature of the sensor between fractions of degrees up to several degrees' thermal conductivity can be determined.

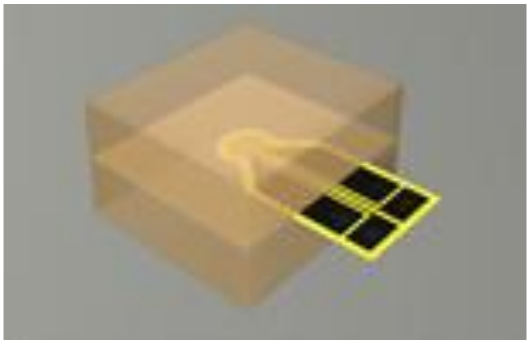

Figure 4: Sensor placement *[48]*

Thermal properties are calculated by recording the temperature increase as a function of time. The Hot Disk sensor is used both as a heat source and as a dynamic temperature sensor. The solution of the thermal conductivity equation assumed that the Hot Disk sensor is located in an infinite medium, which means that the transient recording must be interrupted as soon as any influence from the outside boundaries of the two sample pieces is recorded.

The Hot Disk Thermal Constants Analyzer has been used for studying many different materials such as metals, alloys, minerals, ceramics, glasses, powders, plastics, building materials, biomaterials in vivo or in vitro, liquids etc. The highest temperatures reached so far with specially designed sensors were between 1700 K and 1800 K.

Table 3: The specification of TPS *[48]*

Thermal Conductivity	0.03 to 100 W/m/K using standard isotropic method
Thermal Diffusivity	0.02 to 40 mm^2/s using standard isotropic method
Specific Heat Capacity	0.10 to 4.5 MJ/m^{3}K
Measurement Time	2.5 to 2560 sec
Reproducibility	2 % (thermal conductivity)
Accuracy	Better than 5 % (thermal conductivity)
Sensor Types Available	Kapton sensors: 7577, 5465, 5501

3.2.1 Working of TPS 500S with Fluids:

The TPS 500 S is capable of finding the thermal transport properties of isotropic materials. To begin the experiment, the following inputs are required: measurement time [Sec], heating power [Watts], test sample temperature [^{o}C], sensor type, sensor material type, sensor design, probing depth, start point, and end point

Figure 5:Liquid cell to hold nanofluid

Table 4: The ideal values of the input parameters for liquids

Input Parameters	Range
Measurement Time	10 secs
Heating Power	10-25 mWatts
Test Sample Temperature	Ambient temperature
Sensor Type	Disk
Sensor Material Type	Kapton
Sensor Design	7577, radius 2.0 mm; maximum radius to be used is 3.2
Probing depth	2-3 mm
Start Point	10
End Point	200

TPS 500S can be turned on by flipping the switch on the back side of the unit. The unit should be turned on 60 minutes prior to the experiment. Input all the input parameters and click “start” to begin the experiment. The TPS 500S heats the sample with the selected power and at the same time record 200 data points of the temperature increase of the sensor.

This recording of temperature increase is known as transient recording. Two graphs: drift graph and transient graph are displayed when transient recording is completed.

Drift Graph: Drift graph displays measured sensor temperature increase before heating. In the graph x-axis is time [sec] and y- axis is temperature increase [k]. The measured sensor temperature increase before heating should show small variations. If the sample is still cooling down from the previous experiment this would show on this graph. The experiment should be performed when the sample is isothermal and there is no temperature drift present.

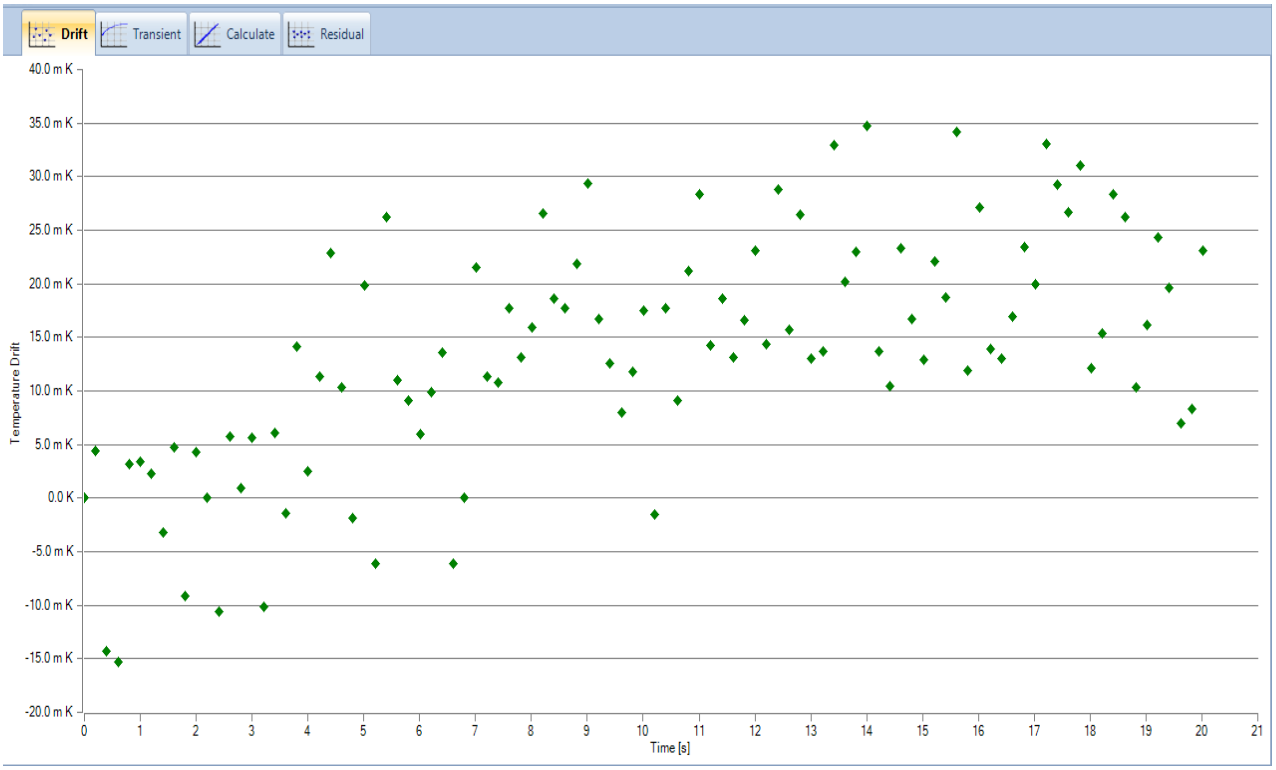

Figure 6: Drift graph *[48]*

Transient graph: It is a temperature increase vs time [sec] graph. Graph displays the measured sensor temperature while heating the sample. It shows all the 200 points which are recorded to calculate the thermal properties of the sample.

After the transient recording is completed and a drift graph and a transient graph are displayed; click on the “Calculate” button to find the thermal properties of the liquid. Enter the start point as “10” and end point as “200” and click on “standard analysis”. The thermal properties are calculated and presented in the main window under experiment tab.

The results are as follows:

A Calc temperature/ F (tau) graph, a Residual graph and Numeric results.

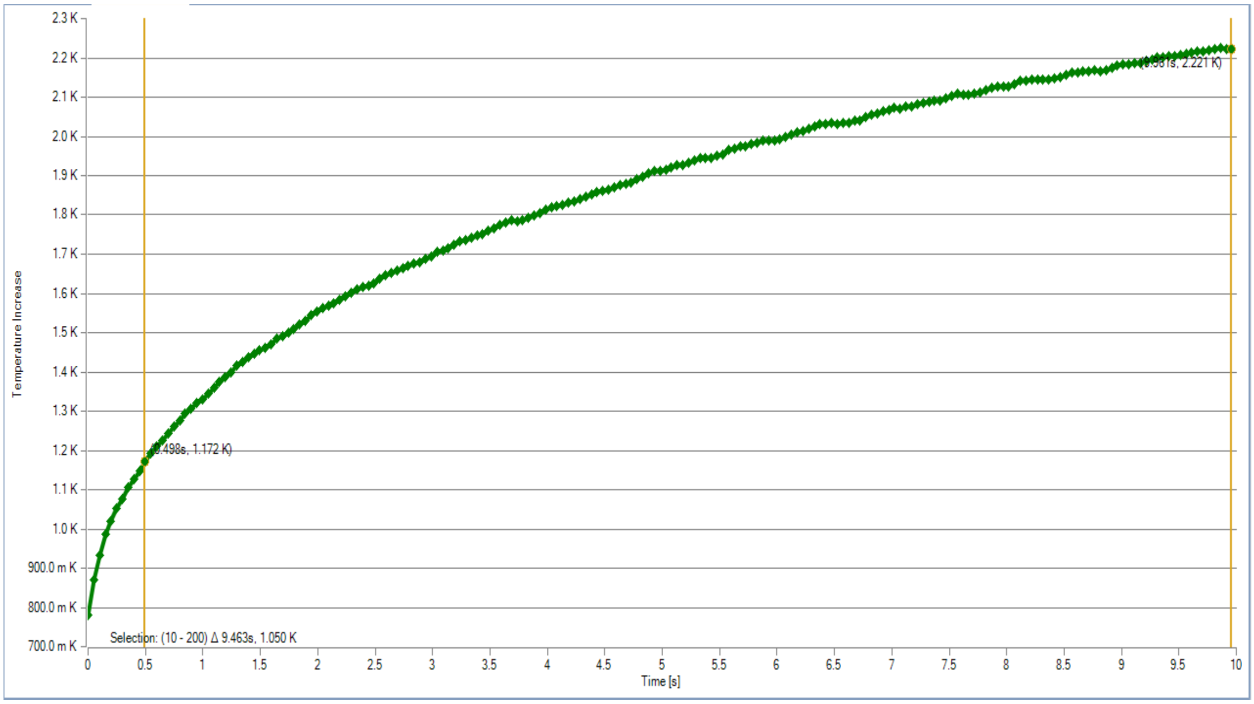

Figure 7: Transient graph *[48]*

Calc graph: Displays temperature increase versus F (T). The temperature can be expressed as a linear function of a dimensionless time function F (T). From the slope of this straight line, the thermal conductivity can be calculated.

As the Hot Disk is electrically heated, the resistance increases as a function of time is given by:

$$R(t) = R_o \{1+ \alpha\{.[\ T_i+\Delta T_{ave}(T)]\} \tag{19}$$

$$\Delta \mathrm{Ti} + \Delta \mathrm{Tave}(\mathrm{T}) = \frac{1}{\alpha}\left(\frac{R(t)}{R_o} - 1\right) \tag{20}$$

The blue curve indicates the temperature increase of the sensor itself and the red one show how the temperature of the sample surface is increasing.

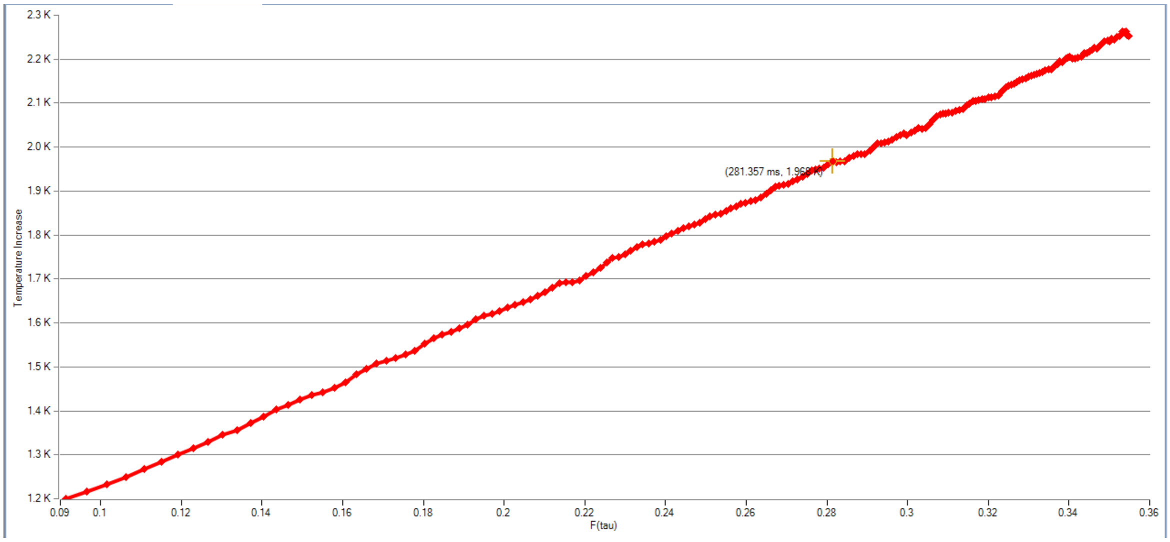

Figure 8: Calculate graph *[48]*

ΔT_i becomes constant after a very short time Δt_i which can be estimated as:

$$\Delta t_i = \frac{\delta^2}{\kappa_i} \tag{21}$$

$$\Delta \mathrm{Tave}(\mathrm{T}) = \frac{P_o}{\pi^{\frac{3}{2}}.a.\Lambda}.F(\mathrm{T}) \tag{22}$$

$$\mathrm{T} = \sqrt{\frac{t}{\phi}} \tag{23}$$

$$\phi = \frac{a^2}{\kappa} \tag{24}$$

Now, by making a computational plot of the recorded temperature increase versus F(T), we get a straight line, the intercept of which is ΔT_i and the slope is $\frac{P_o}{\pi^{\frac{3}{2}}.a.\Lambda}$ using experimental times much longer than Δt_i.

Since κ and hence ϕ are not known before the experiment, the final straight line from which the thermal conductivity is calculated is obtained through a process of iteration. Thus, it is possible to determine both the thermal conductivity and thermal diffusivity from one single transient recording.

Residual Graph: It is a graph of temperature difference versus square time. It gives random scatter of the data around the straight line. If the scatter is not random a new set of data points should be selected for a recalculation.

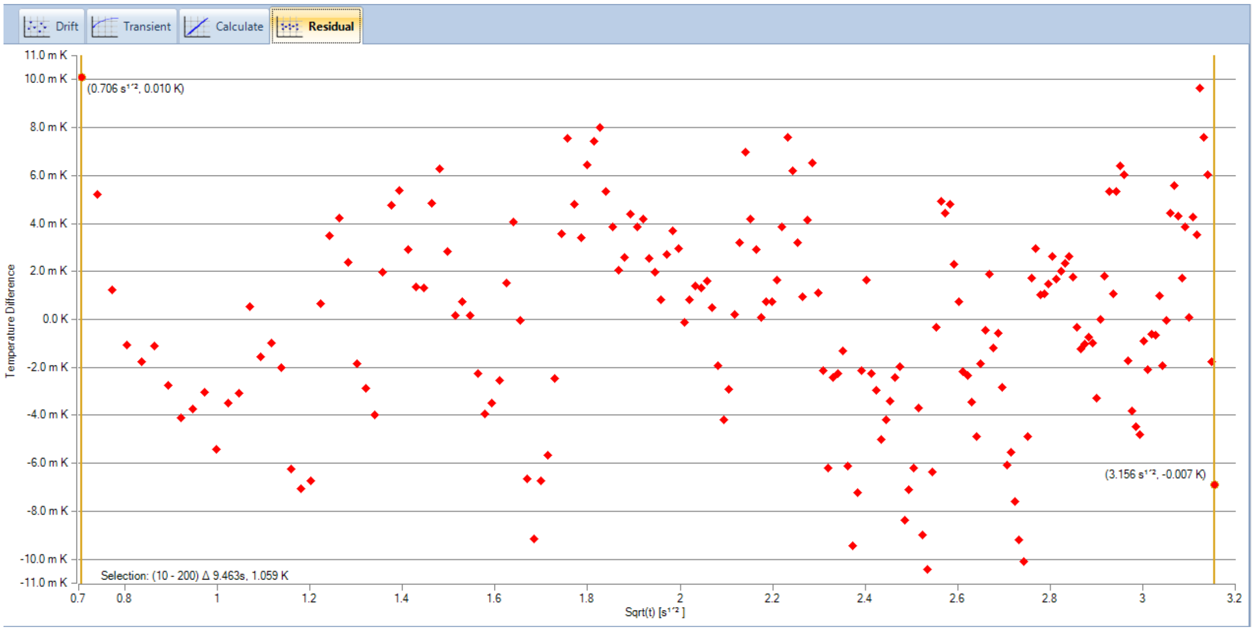

Figure 9: Residual graph *[48]*

3.2.2 Probing Depth:

The important assumption on which the solution of thermal conductivity equation is based is that the sensor is in an infinite material. This means the total time of the transient recording is limited by the presence of the outside boundaries or limited size of the sample. In other words, the "thermal wave" or "thermal penetration depth" generated in an experiment must not reach the outside boundaries of the sample pieces during the transient recording. An estimation of how far this thermal wave has proceeded in the sample during a recording is the so-called probing depth.

$$\Delta_p = 2.\sqrt{\kappa . t} \tag{25}$$

The relation between the probing depth and the total measuring time of the experiment indicates that it is easier to make measurements on larger samples. In order to determine both thermal conductivity and thermal diffusivity with good accuracy, the thickness of a flat sample should not be less than the radius of the hot disk sensor.

3.3 Fast Fourier Transformation:

The fast Fourier transform is a mathematical method for transforming a function of time into a function of frequency. It is also described as transforming a function of time into a function of frequency [49], [50]. It is very useful for analysis of time- dependent phenomena.

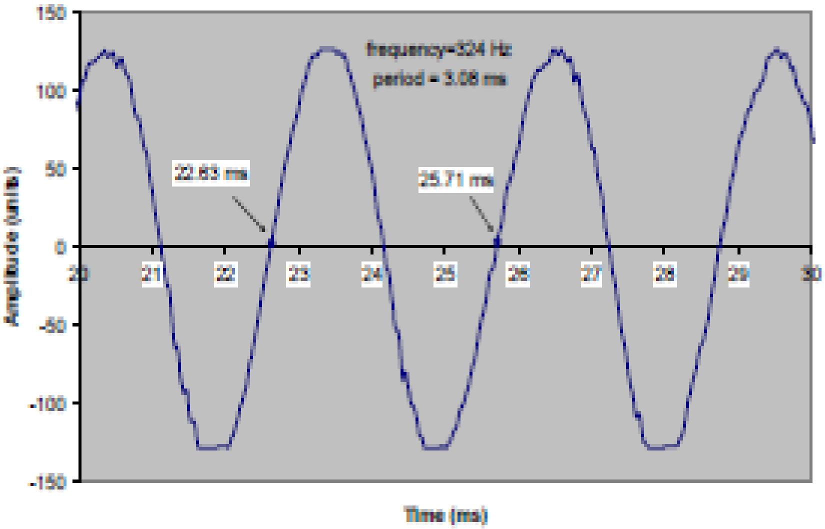

Figure 10: Data in Time Domain [51]

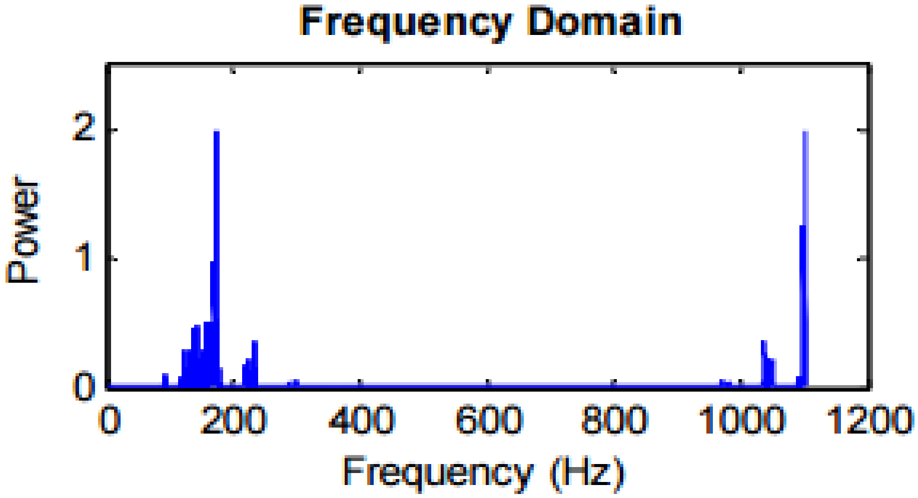

Figure 11: Data in Frequency Domain [51]

Error! Reference source not found.10 displays the magnitude of the waveform versus frequency. It is also called as a frequency spectrum. It provides a visual for a waveform according to its frequency content. Excel and Mat lab can be used to convert the function of time into a function of frequency.

Mathematical calculation of settling velocity, Brownian motion and thermophoresis is possible. The diameter of particle is considered as 10 nm; the base fluid is propylene glycol and nanoparticles are mixed in the volumetric concentration of 0.2%, 2%, and 3%.

3.4 Velocities Calculations:

Settling velocity, Brownian motion and thermophoresis velocities were calculated by using the formulas in *Hind book*. The velocities were as following:

Table 5: Velocities calculation of nanofluids

SnO	Vol. Concentration	Settling Velocity (cm/sec)	Brownian motion (cm/sec)	Thermophoresis (cm/sec)
1	0.2%	1.11E-09	3.30E-17	1.69E-07
2	2%	1.05E-09	3.13E-17	1.69E-07
3	3%	1.05E-09	3.12E-17	1.67E-06

From the Table *5*, it can be concluded that the effect of thermophoresis is at its maximum in the nanofluid when the nanoparticle used was Al_2O_3, the diameter used was 10 nm, and the base fluid was propylene glycol.

Chapter 4: Experimentations

4.1 Calibration of TPS 500S:

Before mixing the nanoparticles in base fluid, the task was to calibrate TPS 500S with fluids with known thermal conductivity. The fluids chosen were distilled water and propylene glycol. The thermal conductivity of distilled water and propylene glycol is 0.591 W/m.K and 0.206 W/m.K respectively [52], [53]. Three important inputs were added into TPS software to start the experiments. The inputs were: input power, experiment time, and probe depth. For liquids, the input power should be a small value to avoid natural convection.

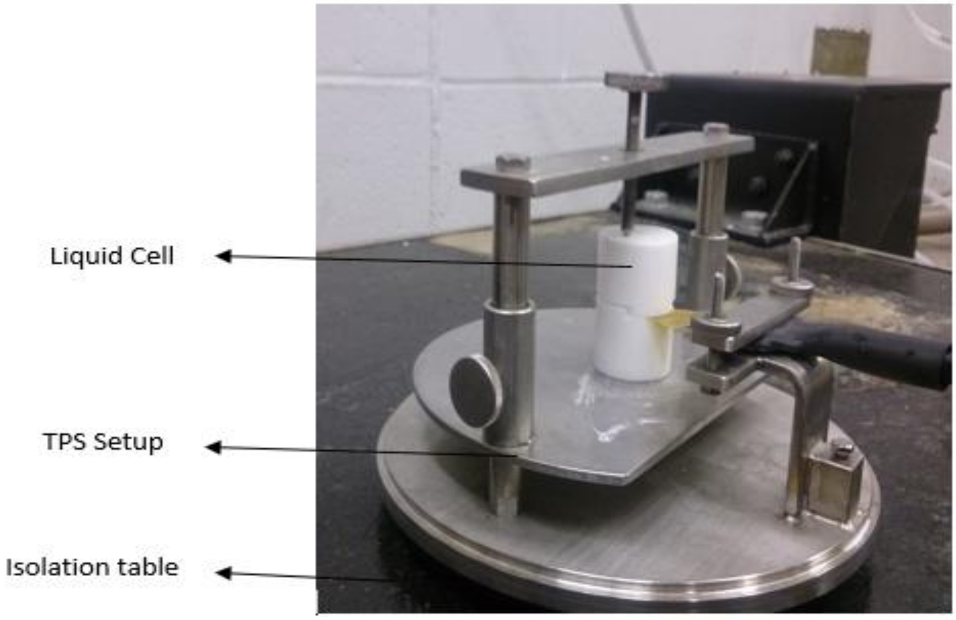

Figure 12: TPS 500S setup

4.2 Experiments with Distilled Water:

The aim of the experiments was to calibrate the TPS 500 S by using distilled water. The standard value of thermal conductivity is published in many papers [53]. Input power, experiment time, and probe depth were kept as 10 mwatt, 10 secs, and 1.5 mm, respectively.

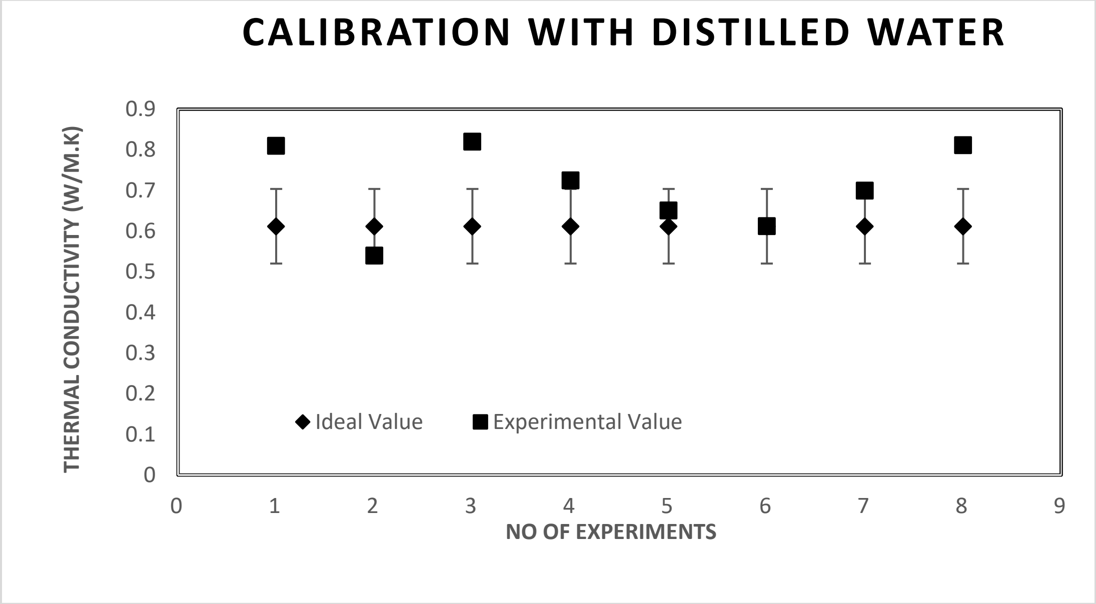

Figure 13: Calibration with distilled water with parameter as 10 mwatt, 10 secs and, 1.5 mm

From the experiment’s results, it was evident that the results were not constant. There was a huge variance in the experiment data when it was compared with the ideal value. The next step was to conduct the experiments again with different input parameters.

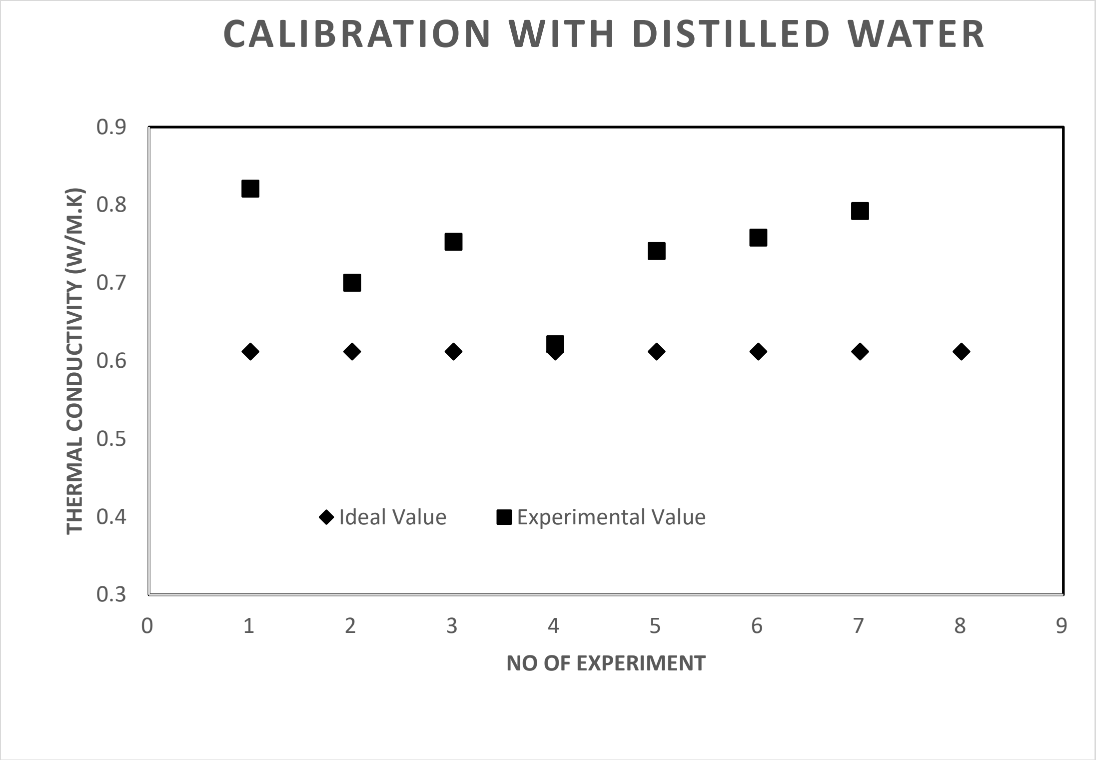

Figure 14: Calibration with distilled water with parameters as 15 mWatt, 10 secs, and 1.5 mm

The results from the experiments showed a high variance. The reason for the variance could have been attributed to either electrical vibrations or mechanical vibrations around the setup. Another approach to eliminate noise in the experiment was to calibrate the equipment by adding specific heat value of the sample. TPS 500 S has the option of taking in the input of the sample's known specific heat to be tested. Another experiment was conducted in which the specific heat of the water was inputted.

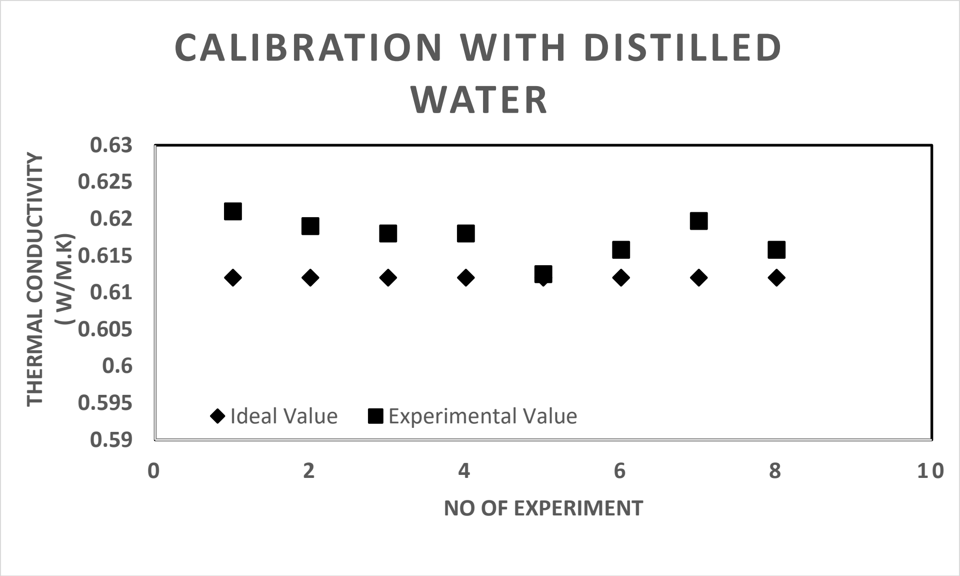

Figure 15: Calibration with distilled water with input value of specific heat

When the specific heat was added as an input parameter, standard deviation and variation reduced significantly. However, the specific heat of nanofluids would have been unknown, and it seemed like crafting the experiments to achieve the reduction in noise. Hence, this approach was neglected. Further experiments were conducted to understand the standard deviation in the calibration process. In the next step, experiments were conducted with propylene glycol to investigate if a similar pattern of noise in experiments was visible in results.

4.3 Calibration with Propylene Glycol:

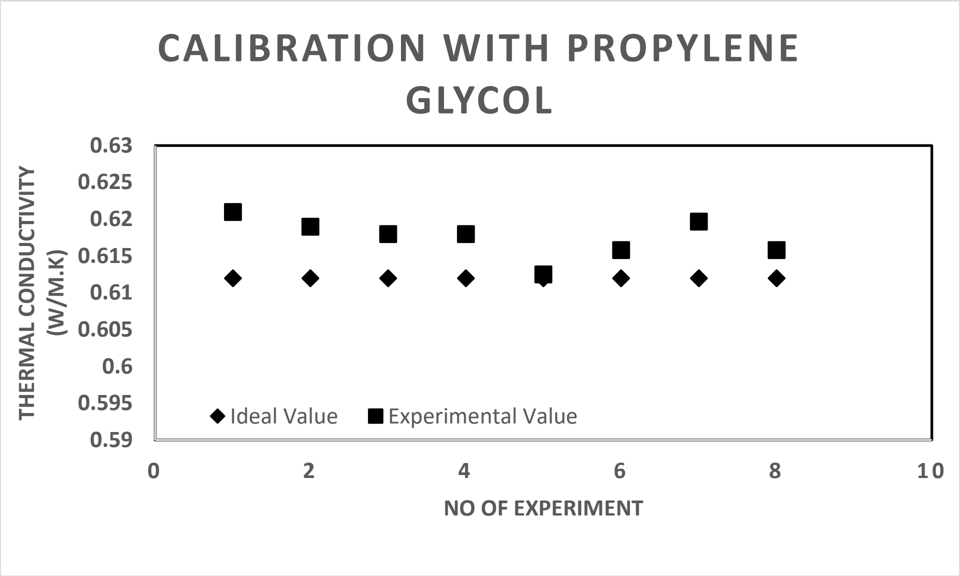

Figure 16: Calibration with propylene glycol

A similar deviation problem was observed in the experiment results when the experiments were done with propylene glycol. The next step was to understand the reason of deviation in the experiments. Fast Fourier Transformation (FFT) analysis was conducted on the data to find out if any predominant frequencies were in the data.

4.4 FFT Analysis and Isolation Table:

To understand the noise in the experiment, FFT analysis was done on the data. Excel was used to do the FFT analysis [51].

The graph is as following:

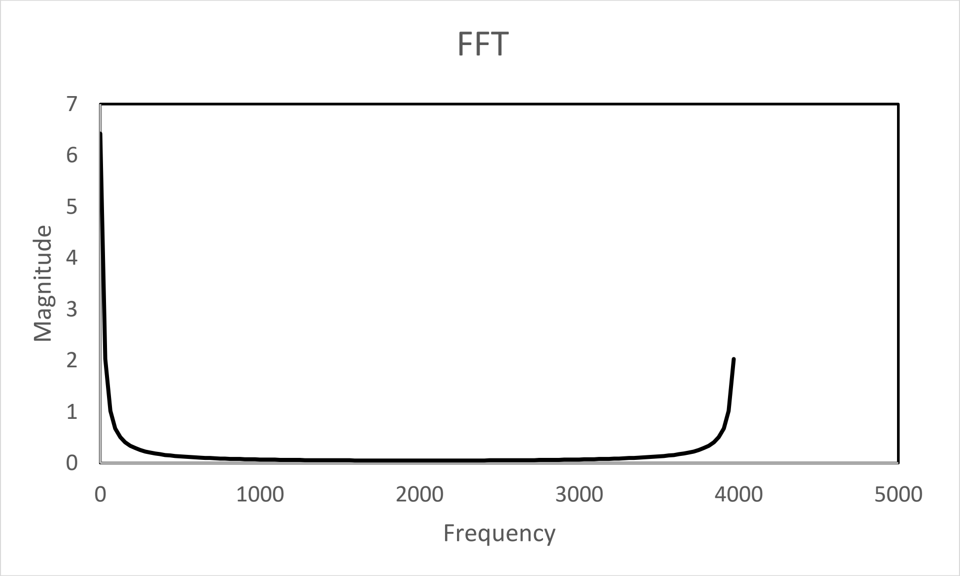

Figure 17: FFT analysis on TPS data

The signals from TPS were small and not harmonic in nature. No predominant frequency showed up in the FFT analysis.

Another approach used was to use an isolation table to remove the unwanted noise in the experiments. Figure *18* shows the isolation table with TPS 500S being placed on it.

Figure 18: Isolation Table with TPS setup on it

For the isolation table, there were three chambers. This chambers were pumped with compressed air. Compressed air lifted the isolation table above the ground and isolated any mechanical vibrations. For our experiments, the pressure in the isolation table was to be kept between 15 Ksi to 20 Ksi. Compressed air was to be pumped constantly to the isolation table. Again, experiments were conducted to see the effects of the isolation table on the results.

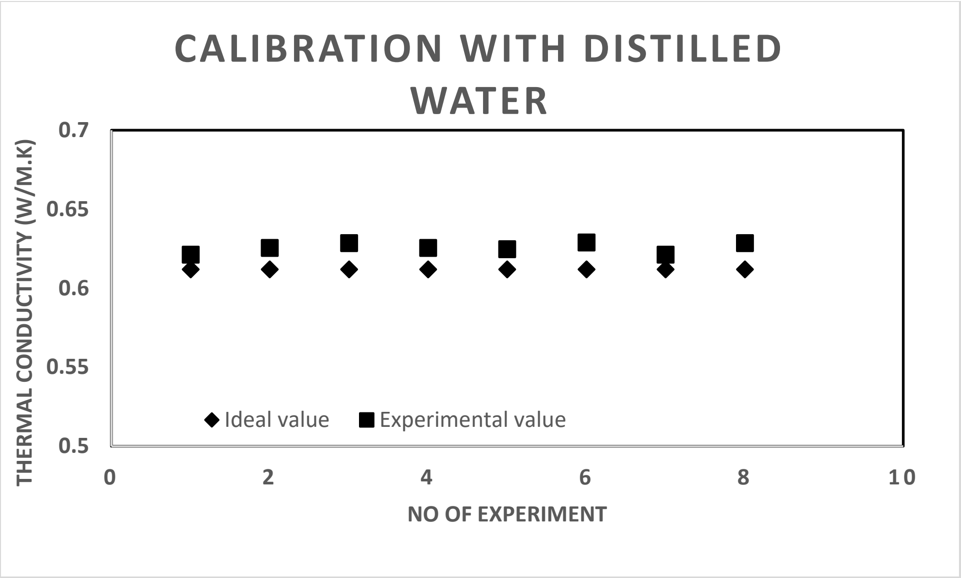

Figure 19: Calibration of TPS 500S with Distilled Water on isolation table

Clearly, standard deviation decreased significantly as compared with the previous experiment. Similar experiments were repeated on propylene glycol to verify the repeatability of the results. The results of experiments conducted on propylene glycol were as following:

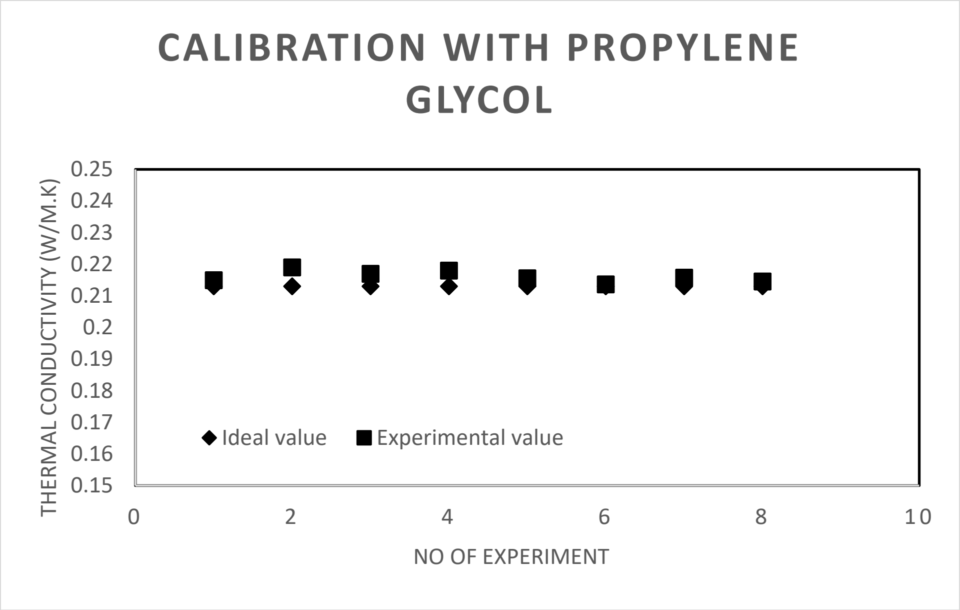

Figure 20: Calibration of TPS 500S with propylene glycol on isolation table

The calibration of TPS 500 S, when conducted on isolation table, gave consistent and reproducible results. The next step was sample preparation. The samples were prepared by mixing Al_2O_3 nanoparticles in propylene glycol.

4.5 Sample Preparation:

The preliminary step for the experiment was the preparation of nanofluids. To obtain accurate results, proper and careful preparation of nanofluids was required. Nanofluids were correctly prepared when there was negligible agglomeration of particles and particles were well dispersed. The aim of the experiments was to study the stability of nanoparticles in a base fluid and also to study the effects of Brownian motion and thermophoresis on the thermal conductivity of nanofluids. To study this, the volumetric concentration of the nanoparticles was kept below 3%. By doing so the coagulation was also minimized.

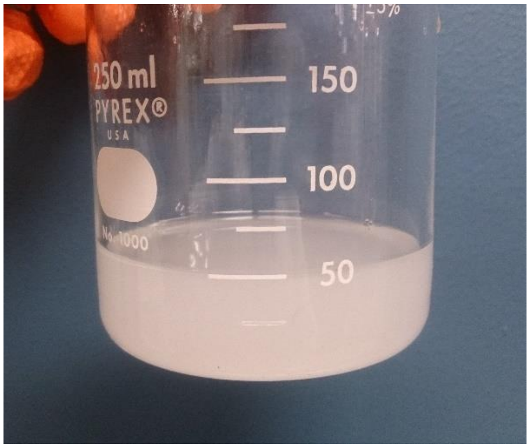

Figure 21: Well stirred Al_2O_3/PG nanofluid

To study the stability of nanofluids and the effects of settling on nanofluids, three different mixtures of fluids were made. The base fluid of propylene glycol was mixed with Al_2O_3 nanoparticle that had a diameter 10 nm. Nanofluids of three different volumetric concentration- 0.2%, 2% and, 3% were prepared in a 50 ml beaker.

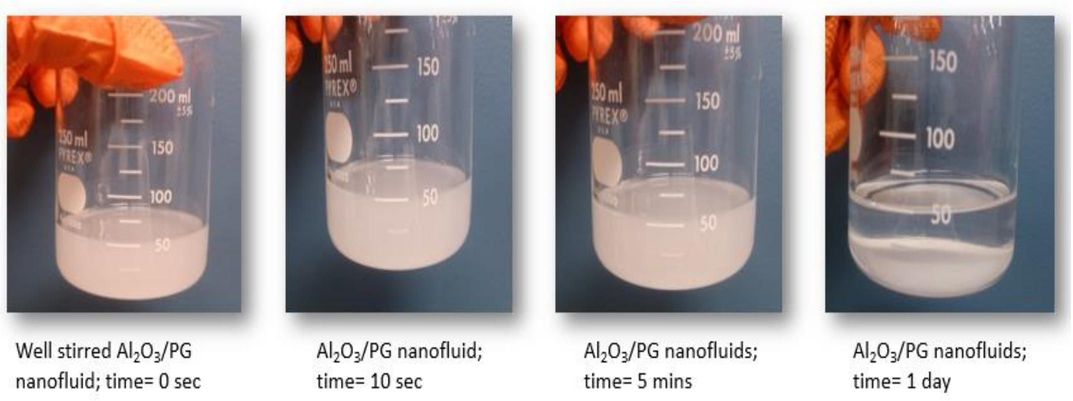
Well stirred Al_2O_3/PG nanofluid; time= 0 sec

Al_2O_3/PG nanofluid; time= 10 sec

Al_2O_3/PG nanofluids; time= 5 mins

Al_2O_3/PG nanofluids; time= 1 day

Figure 22:Al_2O_3/PG nanofluid over time

Chapter 5: Results and Discussion

5.1 Results:

To study the effects of settling on the thermal conductivity of nanofluids with three different volume percentage: 0.2% vol. Al_2O_3/ PG, 2% vol. Al_2O_3/PG and 3% vol. Al_2O_3/ PG were tested. Two sets of experiments were made. In one, nanofluids were freshly mixed, and in the other, nanofluids were kept and settled for 24 hours. Both these sets were tested for 0.2% vol. Al_2O_3/ PG, 2% vol. Al_2O_3/PG and 3% vol. Al_2O_3/ PG of nanofluids. The experiment setup was chosen in this way to study the effect of settling of nanoparticles on thermal conductivity. A total number of 21 experiments were conducted in each set, with an interval of 20 mins in each experiment. The interval of 20 minutes was chosen between the experiments to minimize the chance of natural convection.

The results showed that the value of thermal conductivity increased as the volumetric concentration of the nanoparticles increased. Thermal conductivity values increased with time in both the well stirred mixture and settled mixture. This increase was because of the settling of the nanoparticles on the sensor.

The percentage increase in thermal conductivity in 0.2 % volumetric concentration Al_2O_3/ PG nanofluid was 5.746%. The average percentage increase for the settled mixture was approximately 8%. A similar kind of trend was observed in Al_2O_3/ PG nanofluid, 2% volumetric concentration, and 3% volumetric percentage nanofluid. The percentage increase for 2% nanofluid for the well dispersed mixture and the settled mixture were

15.93% and 19.95% respectively. The percentage increase for 3% nanofluids for the well dispersed mixture and the settled mixture was 21.74% and 28.70%, respectively.

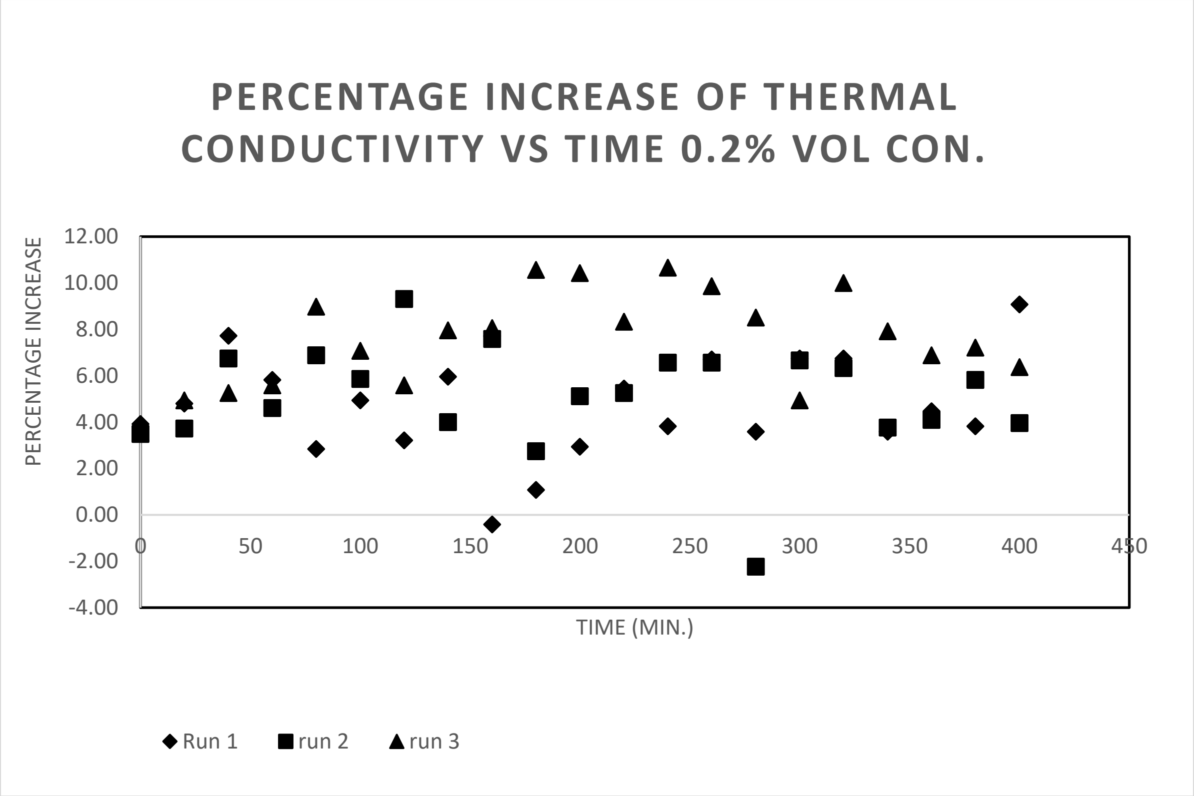

Figure 23: Percentage increase in thermal conductivity, 0.2 % vol. concentration, well stirred mixture

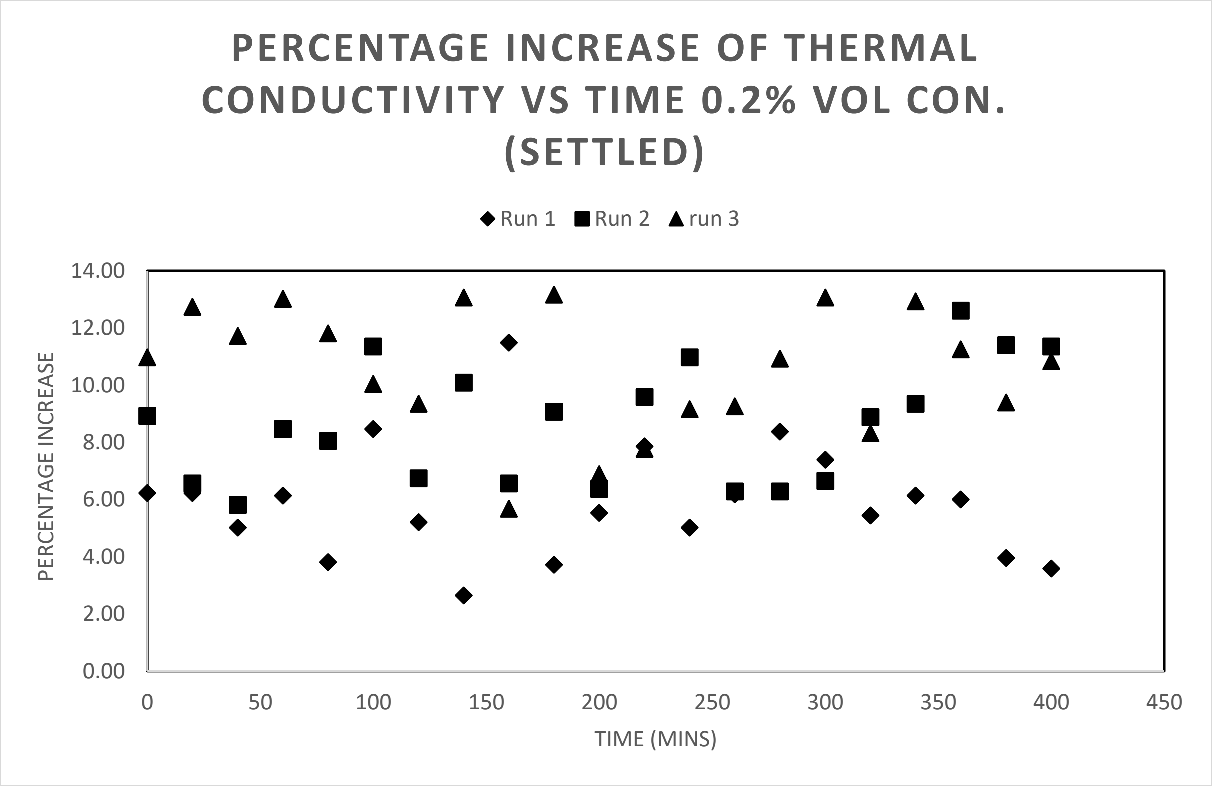

Figure 24: Percentage increase in thermal conductivity, 0.2 % vol. concentration, settled mixture

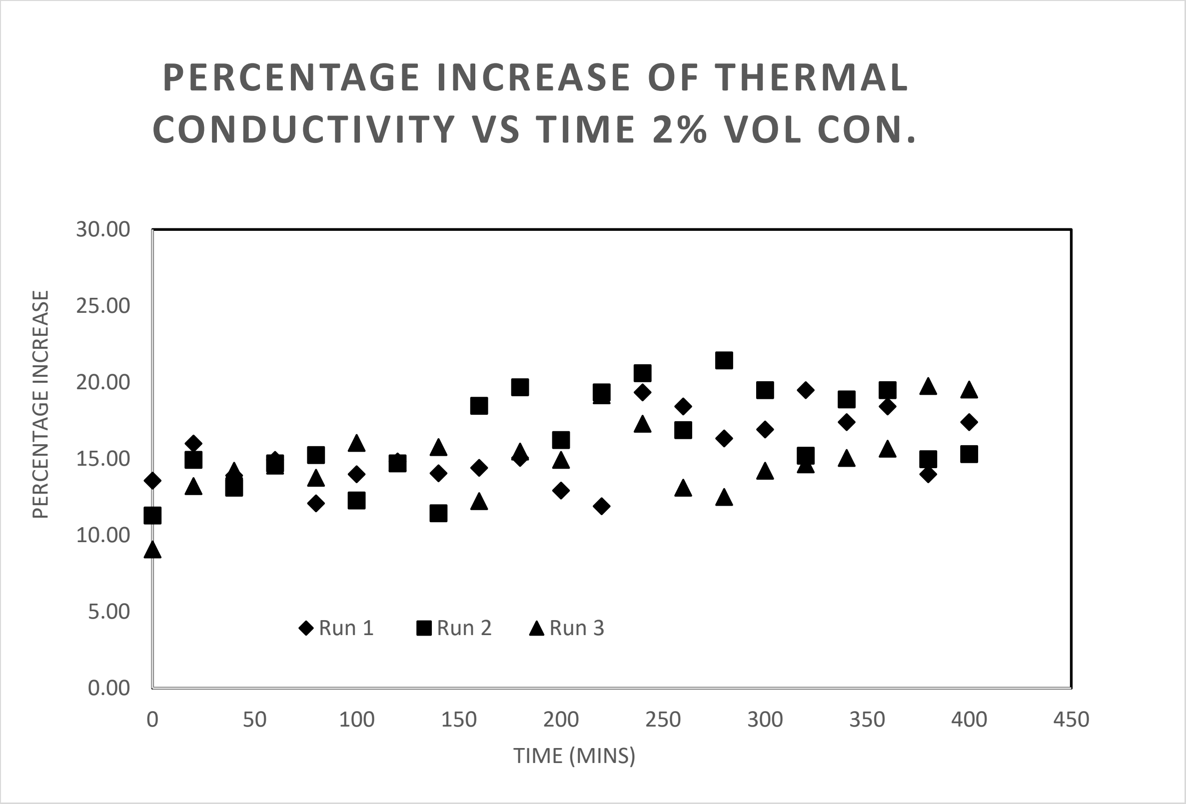

Figure 25: Percentage increase in thermal conductivity, 2 % vol. concentration, well stirred mixture

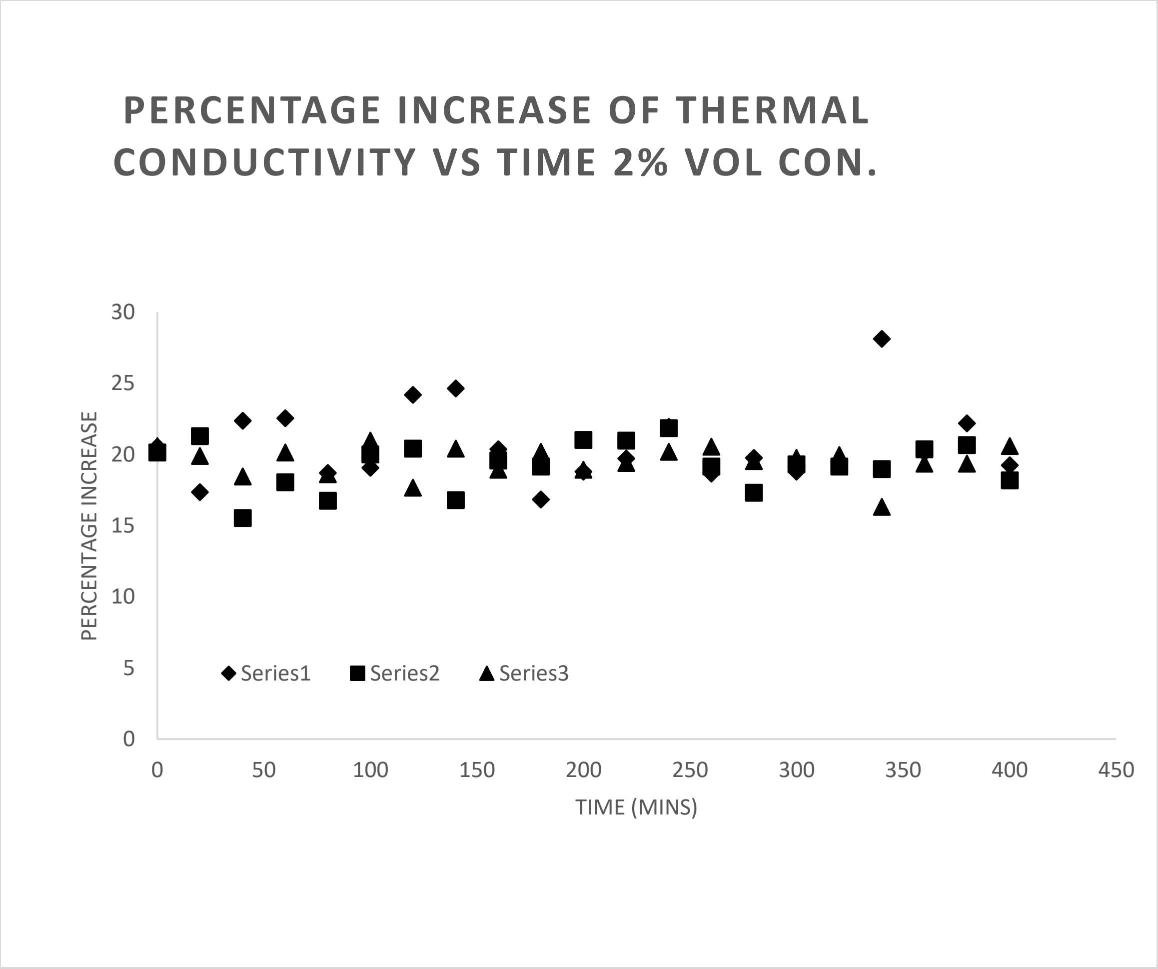

Figure 26: Percentage increase in thermal conductivity, 2 % vol. concentration, settled mixture

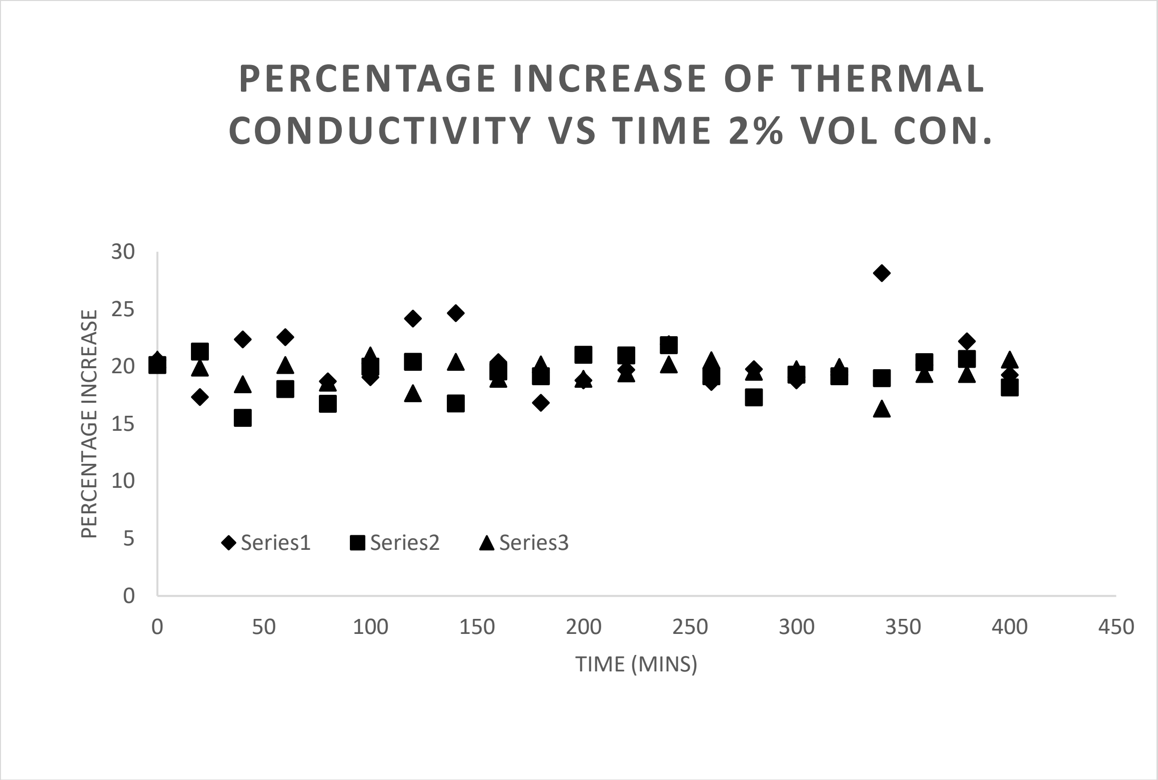

Figure 27: Percentage increase in thermal conductivity, 3 % vol. concentration, well stirred mixture

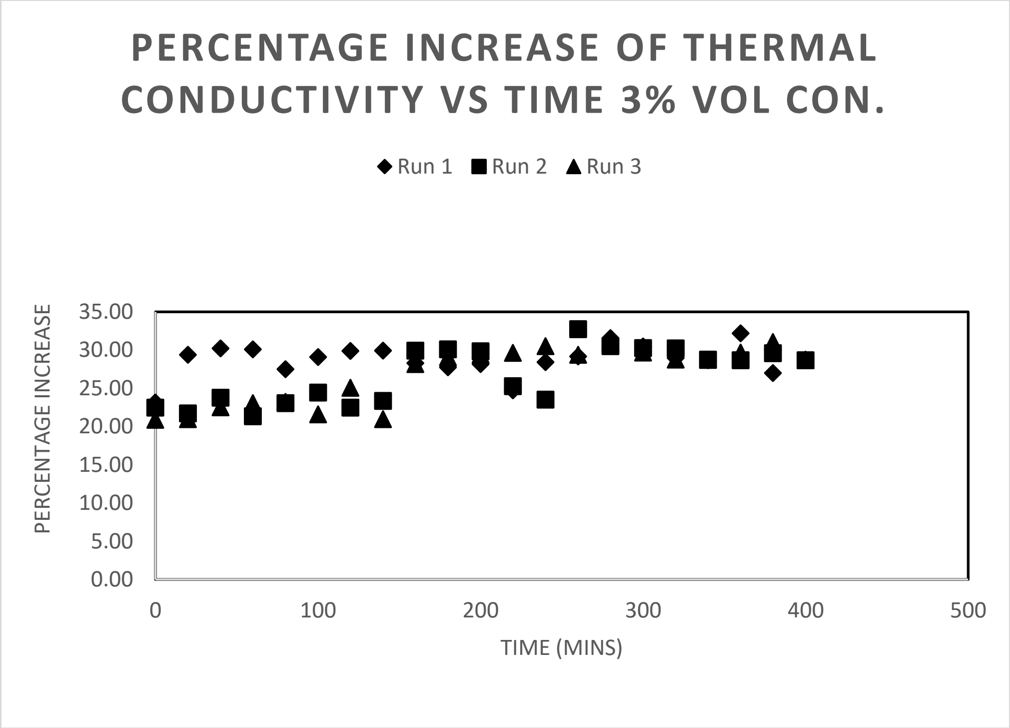

Figure 28: Percentage increase in thermal conductivity, 3 % vol. concentration, settled mixture

The relationship between the well stirred mixture and the settled mixture was studied over time for 0.2%, 2% and 3% mixture. The results showed that the thermal conductivity of the settled mixture was greater than the thermal conductivity of the well stirred mixture in all three cases. From Figure 29, for 0.2% mixture, there was no actual trend in the data. The reason for this behavior could be attributed to the thermophoresis, which might be affecting the settling of nanoparticles. Figure 30 showed the results for the 2% mixture, where the thermal conductivity value of the well stirred mixture rose with time, which gave indication to the settling of the nanoparticles on the sensor. The slope of the 2% settled mixture was smaller than the well stirred mixture's slope. Figure 31 shows the 3% mixture. Both the well stirred and settled mixture's thermal conductivity values were increasing with time. However,the increase in settled mixture was more significant as there was a greater concentration of particles settling on the sensor and creating a thick layer of nanoparticles on the sensor, which might be the reason for this trend.

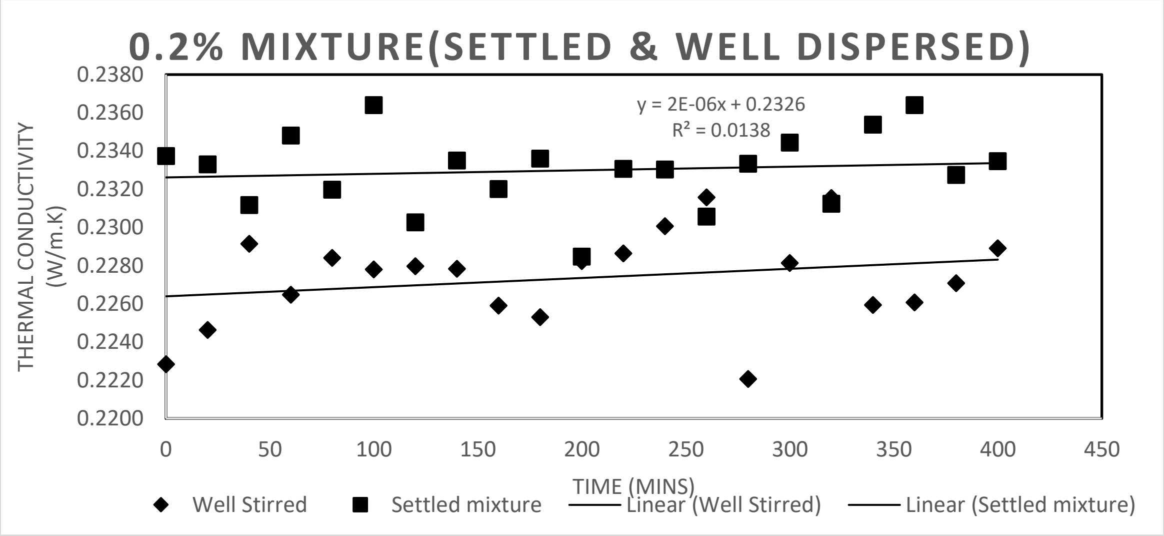

Figure 29:0.2% mixture with time

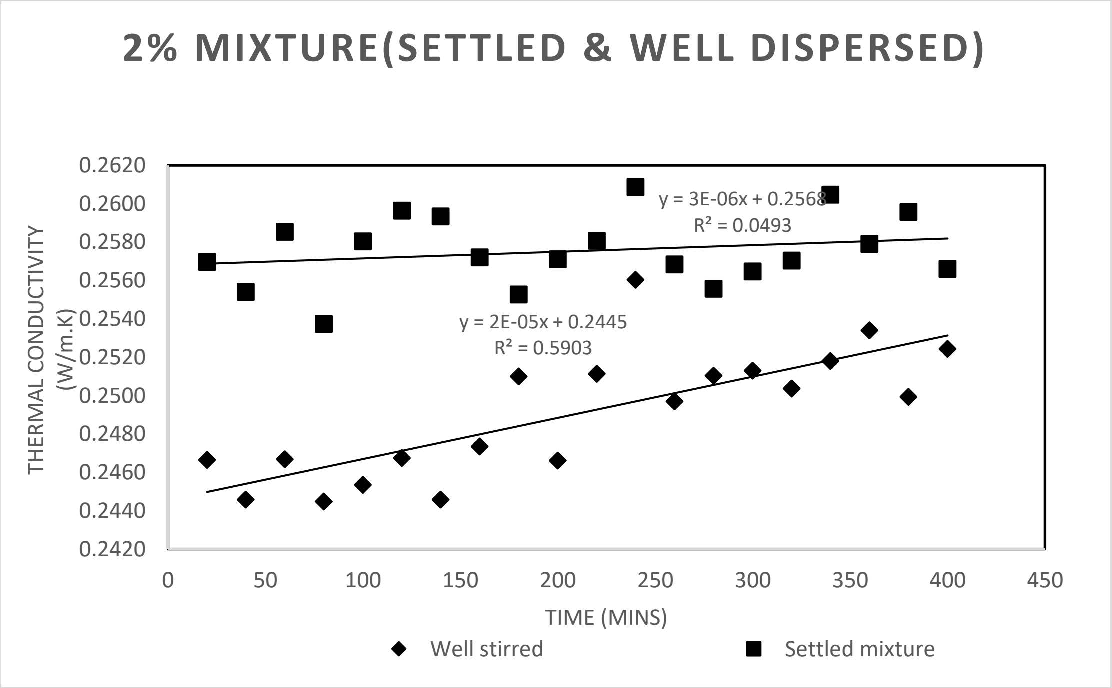

Figure 30: 2% mixture with time

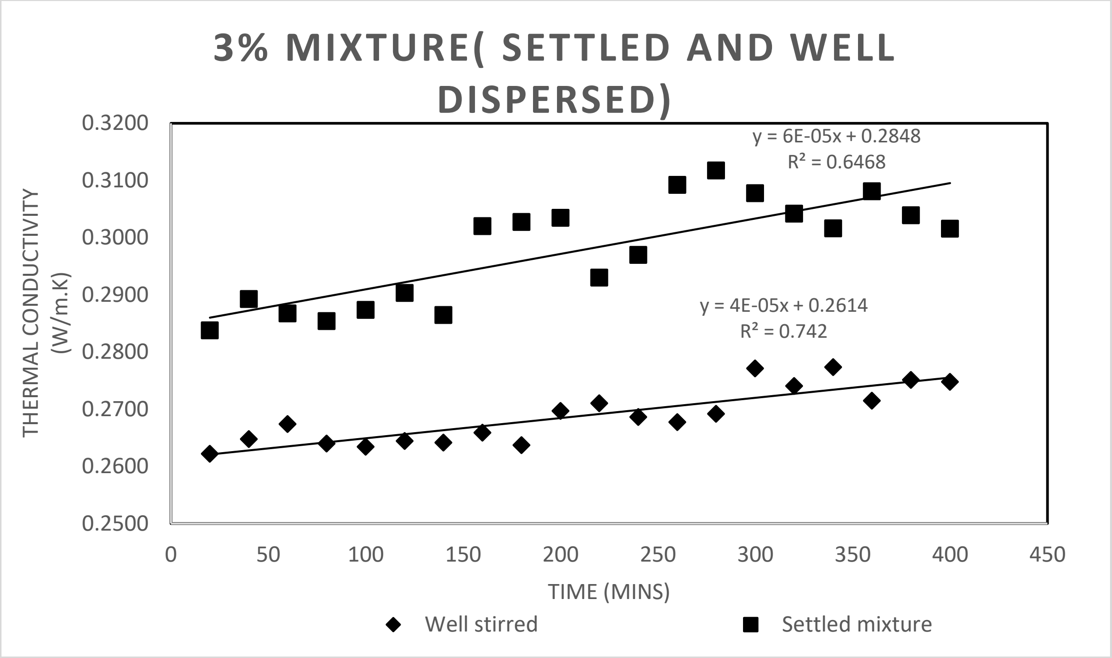

Figure 31: 3% mixture with time

Chapter 6: Summary and Conclusion

6.1 Summary:

All the experimental data showed that the thermal conductivity of nanofluids increased with the addition of nanoparticles. The aim of the experiments was to understand the effect of settling on the thermal conductivity of nanofluids. To study the effects of settling, Brownian motion, and thermophoresis on thermal conductivity, a set of 21 experiments were conducted. The time between each experiment was kept as 20 minutes to ensure that no natural convection happened. Nanofluids were prepared so that the effects of coagulation were minimized, and the effects of settling, Brownian motion, and thermophoresis could be studied.

Two different kinds of experiments were conducted - one in which nanofluids were well stirred and another in which nanofluids were kept at rest for one day and then the experiments were run. For a mixture with a volumetric concentration of 0.2%, a percentage increase of 5.746% and 8.368% were recorded for the well-stirred mixture and the settled mixture, respectively. This trend deviated from the previous studies done by many researchers. Previous studies stated that thermal conductivity decreases with the passage of time. However, in my study the trend showed that thermal conductivity increases with the time, which is opposite to many researches. Similarly, it was noted that thermal conductivity increased with time in the volumetric concentration of 2%, and 3%. For a volumetric concentration of 2%, the improvement in thermal conductivity for the well stirred mixture and the settled mixture was 15.93% and 19.95% respectively. Additionally, for the volumetric concentration of 3%, the improvement was 21.74% and 28.70% for the well stirred mixture and the settled mixture. The reason for this trend was the setup of the TPS 500S. A sensor was placed between the two blocks and liquid was poured from the top block. With time, nanoparticles settled on the sensor, which resulted in an increase in thermal conductivity values.

6.2 Conclusion:

The data collected from experiments was completely opposite from the expected results. The data showed that the thermal enhancement in the settled mixture was greater than in the well-stirred mixture. The results were repeated in all three volumetric concentrations. The results showed that the nanoparticles settled after a passage of time which meant that the nanofluid mixture is not stable with passage of time. Nanofluid behaved as a stable mixture when the volumetric concentration is 0.2%. The reason for that behavior could be attributed to thermophoretic force. The results also showed that a different setup would need to be designed to conduct experiments with the nanoparticles with time. Also, thermal conductivity results changed with time. Hence, the bigger the nanoparticles are, the less time should be taken for the setup and conducting of experiment.

6.3 Recommendation and Future Study:

After carefully analyzing the experimental setup, it was observed that a thin layer of metal oxide was forming on the sensor. Liquid cell was designed in such a way that very little fluid was placed in the cell and the sensor was in between the liquid cell. The deposition of a metal oxide layer explained the higher enhancement of thermal conductivity in the settled mixture than in the well-stirred mixture.

To my knowledge, a different set up of TPS 500S is required to study the effects of settling, Brownian motion and thermophoresis on nanofluids.

Experiment setup could be very simple. A level adjustable sensor in a beaker containing nanofluids could serve as a new setup. The sensor could be kept stationary when the experiments are in the progress. Because of this change in setup, it will be easier to study settling phenomenon at a different level and over time with ease. In addition, a mathematical model could be designed to simulate settling of nanofluids. The mathematical model could calculate the thermal conductivity with the passage of time. Then the data obtained from experiments could be compared with a mathematical model.

Bibliography

[1] Akira Toda, Hisataka Ohnishi, Ritsu Dobashi. 1997. "Experimental study on the relation between thermophoresis and ize of aerosol paricles."

[2] Beck MP, Yuan Y, Warrier P, Teja AS. "The effect of particle size on the thermal conductivity of alumina nanofluids, J Nanoparticle Res 2009."

[3] Beresnev, S. 2010. "Thermophoresis of aerosol particles- A kinetic analysis."

[4] Brock, J.R. n.d. "On the two theory of thermal forces acting om aerosol particles." *journal of colloid science.*

[5] Chan Hee Chon, Kenneth D. Kihm, Shin Pyo Lee, and Stephen U. S. Choi.. "Emperical correlation finding the role of temperature and particle size for nanofluid (Al2O3) thermal conductivity enhancement."

[6] Chen, Shih H. 1991. "Thermophoretic interactions of aerosol particles with constant temperatures."

[7] E. R. Shchukin, A,N. Kabanov. . "Characteristic features of the thermodiffusiophoretic motion of aerosol particles in the vicinity of a catalytically active surface."

[8] E. R. Shchukin, A. N. Kabanov. "Thermodiffusioretic deposition of aerosol particles on cylindrical surfaces."

[9] Eastman, Stephen U. S. Choi and Jeffrey A. "Enhancing thermal conductivity of fluids with nanoparticles."

[10] Efstathios E. Michaelides, Meisen. 1998. "Brownian movement and thermophoresis of nanoparticles in liquids."

[11] F. Schmidt, F. Stratmann. 2004. "An approximation to o calculate the thermophoretic effect on particle deposition."

[12] Fast Fourier Transforms,2010, http://hyperphysics.phyastr.gsu.edu/hbase/math/fft.html

[13] FFT Analysis Dallas,2009, https://www.utdallas.eduFFTandMatLabpdf.

[14] Fedele, Laura. 1991. "Viscosity and thermal conductivity measurements of water-based nanofluids containing titanium oxide nanoparticles."

[15] Guodong Xia, Huanming Jiang, Ran Liu, Yuling Zhai. 1995. "Effetc of surfactant on the stability and thermal conductivity of AL2O3/ deionized water nanofluids."

[16] Hinds, William c. 1994. "Aerosol technology properties, behavior, and measurement of airborne particles by William c. Hinds."

[17] http://web.chem.ucla.edu/~harding/IGOC/P/propylene_glycol.html. .

[18] Huh, Chun. "Measuring modeling the magnetic settling of nanoparticle dispersions."

[19] 2017. *Illustrated Glossary of Organic Chemistry*. http://web.chem.ucla.edu/~harding/IGOC/P/propylene_glycol.html.

[20] Joris T.K. Quik, Iseult Lynch. "Effect of natural organic matter on cerium dioxide nanoparticles settling in model fresh water."

[21] Jose L Castillo, Pedro L Garcia. "Morphological instability of a thermophoretically growing deposit."

[22] K.S. Suganthi, K.S. Rajan. Improved transient heat transfer performance of ZnO–propylene glycol nanofluids for energy management.

[23] Karthikeyan NR, Philip J, Raj B. "Effect of clustering on the thermal conductivity of nanofluids."

[24] Ki- Hyuck Hong, Shin Hyoung Kang. "Three- dimensional analysis of heat transfer and thermophoretic particle deposition in OVD process."

[25] Klingenberg, Larry. "Frequency Domain Using Excel."

[26] Koetsem, Frederik Van. "Stability of engineered nanomaterials in complex aqueous matrices: Settling behaviour of CeO2 nanoparticles in natural surface waters."

[27] Liquid Cooling, 2017 http://www.lytron.com.

[28] Lee, Ji- Hwan.. "Effective viscosities and thermal conductivities of aqueous nanofluids containing low volume concentrations of Al2O3 nanoparticles."

[29] Lifei Chen, Huaqing Xie.. "Properties of carbon nanofluids stabilized by cationic gemini surfactant."

[30] Lixia Zhou, Dunxue Zhu. "A settling curve modeling method for quantitative description of the dispersion stability of carbon nanotubes in aquatic environments."

[31] M. Jahanshahi, S.F. Hosseinizadeh , M. Alipanah , A. Dehghani , G.R. Vakilinejad.. "Numerical simulation of free convection based on experimental measured conductivity in a square cavity using Water/ SiO2 nanofluids."

[32] Mahbubul, I.M. . "Thermal conductivity, viscosity and density of R141b refrigerant based nanofluid."

[33] Marcos Fernández-Garci, José A. Rodriguez. "Metal oxide nanoparticles."

[34] Mirmohammadi, Seyed Aliakbar.. "Investigation on Viscosity, Thermal Conductivity and Stability of Nanofluids Stockholm, Sweden."

[35] Mohammad Hemmat Esfe, Arash Karimipour, Wei-Mon Yan, Mohammad Akbari, Mohammad Reza Safaei, Mahidzal Dahari. "Experimental study on thermal conductivity of ethylene glycol based nanofluids containing Al2O3 nanoparticles."

[36] Mohammed Taghi Zafarani-Moattar, Hemayat Shekaari, Rima Munes-Rast, Roghayeh Majdan-Cegincara.. "Stability and rheological properties of nanofluids containing ZnO nanoparticles, polypropylene glycol and poly (Vinyl pyrrolidone)."

[37] Propylene glycol USP, 2017 www.propylene-glycol.com.

[38] Propylene Glycol Industrial Grade,2015, http://www.dow.com/en-us/markets-and-solutions/products/PropyleneGlycols/PropyleneGlycolIndustrialGradePGI

[39] Peterson, Calvin H. Li and G. P. *The effect of particles size on the effective thermal conductivity of Al2O3- water Nanofluids.*

[40] Philip, John. "Thermal properties of nanofluids."

[41] Prigiobbe, Valentina. "Measuring and modeling the magnetic settling of superparamagnetic nanoparticle dispersions."

[42] Rohit S. Khedkar, Kailas L. Wasewar. "Influence of CuO nanoparticles in enhancing the thermal conductivity of water and monoethylene glycol based nanofluids, International Communications in Heat and Mass Transfer."

[43] S. Maiga, S.J. Palm.. "Heat transfer enhancement by using nanofluids in forced convection flows."

[44] S. Maiga, S.J.Palm.. "Heat transfer enhancement by using nanofluids in forced convection flows."

[45] S.M.S. Murshed, K.C. Leong, C. Yang. *Enhanced thermal conductivity of TiO2-water based nanofluids.*

[46] Sarit Kumar Das, Nandy Putra, Peter Thiesen, Wilfried Roetzel. . "Temperature dependence of thermal conductivity enhancement for nanofluids."

[47] Sedighi, H. M.. "The influence of dispersion forces on the dynamic pull-in behavior of vibrating nano-cantilever based NEMS including fringing field effect."

[48] Shen, Zhi- Bin. "Vibration of single-layered graphene sheet-based Nano mechanical sensor via nonlocal Kirchhoff plate theory."

[49] Sundar, L. Syam.. *Investigation of thermal conductivity and viscosity of Fe3O4 nanofluid for heat transfer applications.*

[50] Talbot, Cheng, R.K. Schefer. 1980. "Thermophoresis of particles in a heated boundary layer." *Journel of fluid mechanics.*

[51] Teja, Tongfan Sun and Amyn S. "Density, Viscosity and Thermal Conductivity of Aqueous Solutions of Propylene Glycol, Dipropylene Glycol, and Tripropylene Glycol between 290 K and 460 K."

[52] "The influence of dispersion forces on the dynamic."

2015. *Thermal Conductivity Measurements.* http://www.hotdiskinstruments.com.

[53] Thomas, L. C. *Heat Transfer Professional version, second edition.* Capstone Publishing Corporation.

[54] Wanuang Li, E. James Davis "The effect of gas and particle properties on thermophoresis."

[55] Xing Zhang, Hua Gu, Motoo Fujii. *Effective thermal conductivity and thermal diffusivity of nanofluids containing spherical and cylinderical nanoparticles.*

Appendix A:

Table 6: Calibration with distilled water, 10mW

Sample	DW	Room Temp	21
Power (mWatt)	10mW	Time (Sec)	10
Sno	Ther Cond (W/m.k)	Diffusivity (mm^2/sec)	Probe Dept (mm)
1	0.6004	0.1889	2.6403
2	0.5421	0.1408	2.3343
3	0.7907	0.307	2.2779
4	0.7076	0.2327	1.8729
5	0.6301	0.22204	2.08393
6	0.6294	0.28211	2.5853
7	0.6857	0.51729	2.8145
8	0.7705	0.2755	0.2974
Average	0.6696	0.2708	2.1133
St. Dev	0.0852	0.1132	0.7950
Uncertainty		0.66960±0.12428	

Table 7: Calibration with distilled water

Sample	DW	Room Temp	21
Power (mWatt)	10mW	Time (Sec)	10
Sno	Ther Cond (W/m.k)	Diffusivity (mm^2/sec)	Probe Dept (mm)
1	0.6004	0.1889	2.6403
2	0.589	0.1254	2.3564
3	0.7782	0.256	2.1245
4	0.7568	0.245	2.1547
5	0.6125	0.2546	2.0145
6	0.6514	0.1245	2.0125
7	0.6325	0.6254	2.456
8	0.6125	0.1256	2.568
Average	0.6542	0.2432	2.2909
St. Dev	0.0727	0.1652	0.2480
Uncertainty		0.65420±0.12428	

Table 8: Calibration with distilled water by adding specific heat value

Sample	DW	Room Temp	2.432
Power (mWatt)	10mW	Time (Sec)	10
Sno	Ther Cond (W/m.k)	Diffusivity (mm^2/sec)	Probe Dept (mm)
1	0.6256	0.41954	2.44
2	0.6235	0.41954	2.432
3	0.6225	0.41956	2.441
4	0.6223	0.41598	2.44
5	0.6228	0.41954	2.432
6	0.6225	0.41954	2.441
7	0.6245	0.41888	2.44
8	0.6231	0.41921	2.442
Average	0.6234	0.4190	2.4385
St. Dev	0.0012	0.0012	0.0041
Uncertainty		0.62374±0.00138	

Table 9: Calibration with distilled water on isolation table

Sample	DW	Room Temp	2.432
Power (mWatt)	10mW	Time (Sec)	10
Sno	Ther Cond (W/m.k)	Diffusivity (mm^2/sec)	Probe Dept (mm)
1	0.6256	0.41954	2.44
2	0.6235	0.41954	2.432
3	0.6225	0.41956	2.441
4	0.6223	0.41598	2.44
5	0.6228	0.41954	2.432
6	0.6225	0.41954	2.441
7	0.6245	0.41888	2.44
8	0.6231	0.41921	2.442
Average	0.6234	0.4190	2.4385
St. Dev	0.0012	0.0012	0.0041
Uncertainty		0.62374±0.00138	

Table 10: Calibration with distilled water on isolation table

Sample	DW	Room Temp	2.432
Power (mWatt)	10mW	Time (Sec)	10
Sno	Ther Cond (W/m.k)	Diffusivity (mm^2/sec)	Probe Dept (mm)
1	0.6256	0.41954	2.44
2	0.6235	0.41954	2.432
3	0.6225	0.41956	2.441
4	0.6223	0.41598	2.44
5	0.6228	0.41954	2.432
6	0.6225	0.41954	2.441
7	0.6245	0.41888	2.44
8	0.6231	0.41921	2.442
Average	0.6234	0.4190	2.4385
St. Dev	0.0012	0.0012	0.0041
Uncertainty		0.62374±0.00138	

Table 11: Calibration with propylene glycol

Sample	DW	Room Temp	21
Power (mWatt)	10mW	Time (Sec)	20
Sno	Ther Cond (W/m.k)	Diffusivity (mm^2/sec)	Probe Dept (mm)
1	0.2213	0.1105	1.556
2	0.2132	0.1374	1.735
3	0.2254	0.1365	1.143
4	0.2292	0.1231	1.74
5	0.2234	0.1238	1.64
6	0.2263	0.1184	1.611
7	0.2219	0.1288	1.68
8	0.2287	1125	1.57
Average	0.2237	140.7348	1.5844
St. Dev	0.0051	397.7032	0.1911
Uncertainty		0.2236±0.0051	

Table 12: Thermal conductivity values of 0.2% Al_2O_3/PG nanofluid, well- stirred

PG 0.2 %			
sno	Run 1	Run 2	Run 3
1	0.2234	0.2397	0.2326
2	0.2253	0.233	0.2256
3	0.2316	0.2295	0.2263
4	0.2275	0.2249	0.227
5	0.2211	0.2298	0.2343
6	0.2256	0.2276	0.2302
7	0.2219	0.235	0.227
8	0.2278	0.2236	0.2321
9	0.2141	0.2313	0.2323
10	0.2173	0.2209	0.2377
11	0.2213	0.226	0.2374
12	0.2267	0.2263	0.2329
13	0.2232	0.2291	0.2379
14	0.2294	0.2291	0.2362
15	0.2227	0.2102	0.2333
16	0.2295	0.2293	0.2256
17	0.2295	0.2286	0.2365
18	0.2227	0.2231	0.232
19	0.2246	0.2238	0.2298
20	0.2232	0.2275	0.2305
21	0.2345	0.2235	0.2287
Avg	0.2249	0.227229	0.23171
St Dev	0.004729	0.005851	0.00404
actual value	0.215		
% rise	6.02141		

Table 13:Thermal conductivity values of 2% Al_2O_3/PG nanofluid, well-stirred

	PG 2%		
Sno	Run 1	Run 2	Run 3
1	0.2442	0.2393	0.2345
2	0.2494	0.2471	0.2434
3	0.2449	0.2432	0.2456
4	0.2471	0.2466	0.2463
5	0.241	0.2478	0.2446
6	0.2451	0.2414	0.2495
7	0.2469	0.2466	0.2467
8	0.2452	0.2396	0.2489
9	0.246	0.2547	0.2413
10	0.2474	0.2573	0.2483
11	0.2428	0.2499	0.2471
12	0.2406	0.2566	0.2562
13	0.2566	0.2593	0.2522
14	0.2546	0.2513	0.2432
15	0.2501	0.2611	0.2419
16	0.2514	0.2569	0.2456
17	0.2569	0.2477	0.2465
18	0.2524	0.2556	0.2474
19	0.2546	0.2569	0.2487
20	0.2451	0.2472	0.2575
21	0.2524	0.2479	0.257
Average	0.248319	0.25019	0.247257
St Dev	0.004903	0.00653	0.005421

Table 14: Thermal conductivity values of 2% Al2O3/PG nanofluid, settled

	PG 2% Settled		
Sno	Run 1	Run 2	Run 3
1	0.2592	0.2583	0.2593
2	0.2523	0.2608	0.2578
3	0.2631	0.2484	0.2547
4	0.2635	0.2538	0.2583
5	0.2552	0.251	0.244
6	0.256	0.258	0.2601
7	0.267	0.2589	0.253
8	0.268	0.2511	0.2589
9	0.2588	0.2571	0.2557
10	0.2512	0.2562	0.2584
11	0.2554	0.2602	0.2557
12	0.2574	0.2601	0.2567
13	0.2622	0.262	0.2584
14	0.2551	0.2562	0.2592
15	0.2575	0.2522	0.257
16	0.2554	0.2565	0.2575
17	0.257	0.2562	0.2579
18	0.2755	0.2558	0.2501
19	0.2583	0.2588	0.2566
20	0.2627	0.2594	0.2567
21	0.2564	0.2541	0.2593
Avg	0.25939	0.256433	0.256443
St dev	0.005751	0.003591	0.003681

Table 15:Comparison of thermal conductivity values of 0.2% well stirred and settled mixture

Time(mins)	**0.2% well stirred (W/m.K)**	**0.2% settled (W/m.K)**
0	0.2228	0.2337
20	0.2246	0.2333
40	0.2291	0.2312
60	0.2265	0.2348
80	0.2284	0.2320
100	0.2278	0.2364
120	0.2280	0.2303
140	0.2278	0.2335
160	0.2259	0.2320
180	0.2253	0.2336
200	0.2282	0.2285
220	0.2286	0.2331
240	0.2301	0.2330
260	0.2316	0.2306
280	0.2221	0.2333
300	0.2281	0.2344
320	0.2315	0.2312
340	0.2259	0.2354
360	0.2261	0.2364
380	0.2271	0.2327
400	0.2289	0.2335
Average	0.2274	0.2330
St Dev	0.002446592	0.001976751
% increase	5.75	8.37

Table 16 Comparison of thermal conductivity values of 2% well stirred and settled mixture

Time (Mins)	**2% well stirred (W/m.K)**	**2% settled (W/m.K)**
0	0.2393	0.2589
20	0.2466	0.2570
40	0.2446	0.2554
60	0.2467	0.2585
80	0.2445	0.2537
100	0.2453	0.2580
120	0.2467	0.2596
140	0.2446	0.2593
160	0.2473	0.2572
180	0.2510	0.2553
200	0.2466	0.2571
220	0.2511	0.2581
240	0.2560	0.2609
260	0.2497	0.2568
280	0.2510	0.2556
300	0.2513	0.2565
320	0.2504	0.2570
340	0.2518	0.2605
360	0.2534	0.2579
380	0.2499	0.2596
400	0.2524	0.2566
Average	0.2486	0.2576
ST Dev	0.003857335	0.001822278
% increase	15.62	19.81

Table 17 Comparison of thermal conductivity values of 3% well stirred and settled mixture

Time	**3% well stirred (W/m.K)**	**3% settled (W/m.K)**
0	0.2633	0.2762
20	0.2622	0.2838
40	0.2648	0.2892
60	0.2674	0.2867
80	0.2640	0.2854
100	0.2634	0.2873
120	0.2644	0.2903
140	0.2641	0.2864
160	0.2659	0.3020
180	0.2637	0.3027
200	0.2697	0.3034
220	0.2710	0.2930
240	0.2686	0.2970
260	0.2677	0.3092
280	0.2692	0.3117
300	0.2771	0.3078
320	0.2740	0.3042
340	0.2773	0.3016
360	0.2715	0.3081
380	0.2751	0.3039
400	0.2748	0.3015
Average	0.2685	0.2967
St Dev	0.004887409	0.01004687
% increase	24.90	38.02

Appendix B:

Efforts were made to study the single sided experiments in the TPS with Al_2O_3/ Propylene glycol nanofluid. However, the efforts were not successful. Single sided experiments could have given deeper insights in the effects of thermophoresis on the nanofluids. Single sided experiments could be performed in two ways: In one approach, gravity would pull the particles down while thermophoresis velocities pushed nanoparticles in an upward direction. In another approach both gravity and thermophoresis would pull the nanoparticles in same direction. By comparing both the results, effect of thermophoresis could be studied. In my study, I had made an attempt to study single sided experiment. I had insulated one side of TPS cell with XPS pink insulation. The recommendation to use XPS pink insulation was made by the researchers at Hot Disk company. I was not able to design a fixture which could eliminated all the natural convection in the experiments. Further work needed to be done in designing a better and more efficient fixture for the experiment.

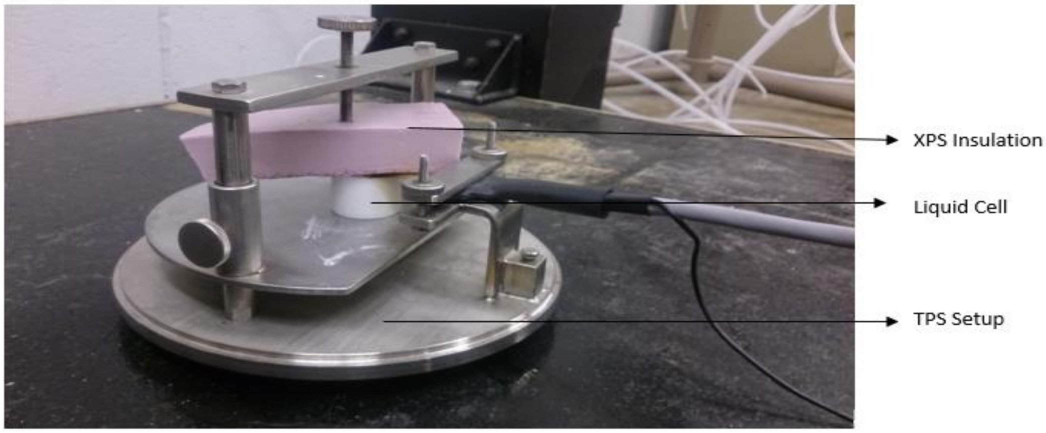

Figure 32 Single sided experiment setup